11-2018

CD147 AS A POTENTIAL THERAPEUTIC TARGET IN GLIOBLASTOMA TREATMENT

Beau Adams
beadams@nmu.edu

CD147 AS A POTENTIAL THERAPEUTIC TARGET IN GLIOBLASTOMA TREATMENT

By

Beau Adams

THESIS

Submitted to
Northern Michigan University
In partial fulfillment of the requirements
For the degree of

MASTER OF SCIENCE

Office of Graduate Education and Research

November 2018

SIGNATURE APPROVAL FORM

CD147 AS A POTENTIAL THERAPEUTIC TARGET IN GLIOBLASTOMA TREATMENT

This thesis by Beau Adams is recommended for approval by the student's Thesis Committee and Department Head in the Department of Biology and by the Interim Director of Graduate Education and Research.

_____

Committee Chair: Dr. Robert Belton Date

_____

First Reader: Dr. Josh Sharp Date

_____

Second Reader: Dr. Robert Winn Date

_____

Department Head: Dr. John Rebers Date

_____

Dr. Lisa S. Eckert Date
Interim Director of Graduate Education

ABSTRACT

CD147 AS A POTENTIAL THERAPEUTIC TARGET IN GLIOBLASTOMA TREATMENT

By

Beau Adams

Glioblastoma (GBM) tumors are the most common and lethal form of cancer in the central nervous system (CNS). GBM tumors appear to contain a mixture of different cell types, which makes them difficult to treat. GBM cells exhibit altered morphology from normal cells on several different levels, which highlights different pathways to potentially target for therapeutic treatments. The human surface glycoprotein CD147, also known as basigin, is expressed at significantly higher levels in GBMs compared to non-neoplastic brain tissue. Furthermore, levels of CD147 expression correlate with brain tumor progression and show the highest expression in GBM. Here, we suppressed tumor cell growth using anti-CD147 monoclonal antibodies. An apoptosis/necrosis assay suggests that GBM cells treated with anti-CD147 monoclonal antibodies were not experiencing a form of induced cell death. Rather, our cell proliferation assay results suggest that anti-CD147 monoclonal antibody treated cells had significantly deceased cell proliferation when compared with control cells. Together, these results show that CD147 is a potential therapeutic target for GBM treatment.

ACKNOWLEDGMENTS

The work presented here would not have been possible without the help of the Upper Michigan Brain Tumor Center, graduate assistantship, summer fellowship, and Excellence in Education grant. I would first like to thank the members of my committee – Dr. Robert Belton, Dr. Robert Winn, and Dr. Josh Sharp for their support and guidance throughout graduate school. I would also like to thank John Lawrence, Amber LaCrosse, Chris McMahon, Rudy Mosca, Colin Smith, Aaron Mellesmoen, Nick Shortreed, and Chris Kyle for their assistance throughout my research project. I have gained more knowledge working in the UMBTC than anywhere else before, and for that I am forever grateful.

This thesis follows the format prescribed by the *American Medical Association Manual.*

TABLE OF CONTENTS

LIST OF FIGURES

LIST OF ABBREVIATIONS

GBM-	Glioblastoma
CNS-	Central Nervous System
ECM-	Extracellular Matrix
KB-	Kilobase
Kda-	Kilodalton
Cav-1-	Caveolin-1
Il-	Interleukin
TNF-α-	Tumor Necrosis Factor Alpha
CSF-1-	Colony Stimulating Factor-1
BM-	Basement Membrane
TGF-β-	Transforming Growth Factor Beta
TkrB-	Tyrosine Kinase Receptor B
EGF-	Epidermal Growth Factor
CTC-	Circulating Tumor Cells
MCT-	Monocarboxylate Transporter
MMP-	Matrix Metalloproteinase
ERK-	Extracellular Signal-Regulated Kinase
VEGF-	Vascular Endothelial Growth Factor
NFKB-	Nuclear Factor Kappa-Light-Chain-Enhancer of Activated B Cells
ATP-	Adenosine Triphosphate
PS-	Phosphatidylserine
DNA-	Deoxyribonucleic Acid
RNA-	Ribonucleic Acid
PI3K-	Phosphoinositide 3-kinase
Akt-	Protein Kinase B
MDM2-	Mouse Double Minute 2 Homolog

Ig-	Immunoglobulin
Fab-	Fragment, Antigen Binding
Fc-	Fragment, Crystallizable
EMEM-	Eagle’s Minimum Essential Medium
FBS-	Fetal Bovine Serum
PSA-	Penicillin-Streptomycin-Amphotericin B
DMSO-	Dimethyl Sulfoxide
mAb -	Monoclonal Antibody
Poly-HEMA-	Poly 2-hydroxyethyl Methacrylate

INTRODUCTION

Glioblastoma (GBM) is the most common and lethal form of primary cancer in the central nervous system (CNS). Glioblastoma is a type of tumor that develops from glial cells, called astrocytes, which function to support nerve cells[1]. Glioblastomas are highly malignant due to their fast growth rates and the extensive blood vessel networks that form near them[2]. During development of the tumor, GBMs appear to contain a mixture of specific differentiated cell types such as oligodendrocytes and ependymal cells. As a result, some GBM cells may respond to specific therapies while others may not respond at all, making GBMs extremely difficult to treat. Despite advances in cancer therapy such as immunotherapy, the prognosis for GBM patients remains poor. Standard GBM treatments include partial removal, chemotherapy, and radiation[3]. Chemotherapy involves the use of drugs intended to kill cancer cells by stopping growth and reproduction. Radiation involves the use of high-energy waves to damage tumor cell DNA, which halts cell division and eventually destroys them. Unfortunately, these treatments are only beneficial for a short period of time and can have negative effects upon the surrounding normal tissues. The survival rate for GBM patients one-year post diagnosis is 33% while the survival rate after five years is 4.5%[4]. Many research laboratories across the world are working to find a potential therapeutic target for GBM to increase the survival rates and improve the treatments of this deadly disease.

The growth and spread of a tumor (called metastasis) involves several steps, including increased cell proliferation, changes in cell motility leading to invasion of surrounding tissues, and the formation of new blood vessels (angiogenesis). The process of angiogenesis ensures that metabolically active tissues, including cancer, are never more than a few hundred micrometers away from capillaries[5]. Angiogenesis is stimulated when vascular endothelial growth factor (VEGF) binds to tyrosine kinase receptors (VEGF-Rs), which then leads to activation of several downstream pathways that regulate angiogenesis. Capillaries are crucial for the process of nutrient/metabolite exchange and provide tissues with a consistent oxygen supply to metabolize substrates that are needed for energy[6]. This is important because cancer cells require this nutrient/metabolite exchange in order to survive[7]. Anti-angiogenic therapies designed to prevent the growth of new blood capillaries are used to combat several diseases, including cancer. These 'angiogenesis inhibitors' generally block the activation of VEGF receptors. The drugs bind to either VEGF and/or VEGF-Rs, blocking receptor binding and subsequent activation of downstream signaling[8]. Angiogenic inhibitors have shown promise in GBM patients but unfortunately exhibit a high percentage of relapse, which calls for a larger understanding of the mechanisms involved in tumor growth.

Rapidly proliferating cells can become resistant to the body's normal defenses, and some can evade endogenous cell death programs designed to prevent unwanted cell growth[9]. Normally, cytotoxic and helper T cells inhibit cancer development through production of cytokines and cytotoxins[9]. However, things such as chronic inflammation can override these effects to promote cancer. When acute immune responses fail to eliminate cancer cells, unresolved chronic inflammation promotes tumor cell growth and

angiogenesis[9]. The human immune system is normally capable of eliminating cancer cells that express mutated proteins (neoantigens), which are molecules encoded by tumor-specific mutated genes. However, increases in cancer cell proliferation also generates cells that can evade immune responses, allowing some cancer cells to escape immune system elimination[9]. Increased cell proliferation leads to the production of immune suppressive cytokines, either by tumor cells or normal cells present in the tumor microenvironment. These cytokines, such as TNF-alpha, IL-1, and IL-6 assist in the evasion of immune surveillance by weakening T cell response[9]. For example, TNF-α promotes cell survival via TNFR1 through its activation of specific transcription factors, which cause downstream activation of the PI3K/Akt/MDM2 pathway (expanded upon in the following pages)[10]. IL-1 induces expression of metastatic genes involved in tumor progression such as VEGF, TNF-α, and other interleukins[11]. IL-6 protects tumor cells from oxidative stress, DNA damage, and apoptosis by facilitating signaling pathways involved in cell survival, which also includes the PI3K/Akt/MDM2 pathway[12].

Another dangerous property of GBMs is their ability to invade nearby tissues, leading to another obstacle of treatment. A good way to summarize this process is the invasion-metastasis cascade[13]. This cascade occurs when primary tumor cells invade the surrounding extracellular matrix (ECM) followed by invasion of the lumina of blood vessels, where tumor cells can be transported through the vasculature. Finally, the tumor cells can move into the parenchyma of distant tissues and then reinitiate their proliferation. These invasive properties contribute to tumor survival and induce molecular changes that maximize metastasis[13]. An understanding of this process is critical for the development of new techniques to diagnose and treat GBM. The first step

in the metastatic process is local invasion, which refers to cancer cells from the primary tumor entering adjacent tissue. In order to invade the tissue, cancer cells must penetrate the basement membrane (BM), a special type of extracellular matrix that separates epithelial and stromal components[10]. From here, these cancer cells must invade lymphatic and blood vessels (intravasation). Intravasation occurs when molecular changes allow these cancer cells to cross endothelial cell barriers that make up blood vessel walls. Examples of molecules promoting intravasation include transforming growth factor-β (TGFβ), epidermal growth factor (EGF), and colony stimulating factor-1 (CSF-1)[14]. Once cancer cells have intravasated into blood vessels, they become circulating tumor cells (CTCs) and must survive to successfully metastasize. In the absence of any anchorage, normal cells in circulation would usually go through anoikis – a type of apoptosis due to loss of anchorage. Cancer cells are able to overcome anoikis due to specific molecules such as tyrosine kinase receptor B (TrkB) that assists in suppression of the immune response[15]. In a study by Douma et al., it was shown that TrkB activates the phosphatidylinositol-3-OH kinase/protein kinase B pathway which induced formation of cellular aggregates that survived in suspension – therefore overcoming anoikis[15]. Eventually, the CTCs arrest at specific sites and begin to invade the walls of surrounding vessels, making direct contact with tissue parenchyma. This process is known as extravasation[13]. In a recent study by Gao et al., CTCs were identified in 77% of glioblastoma patients[16]. CTCs are thought to be one of the main reasons for tumor recurrence in many forms of cancer, including GBM[17].

An example of a molecule that may be involved in all of these tumor-promoting properties is the human surface glycoprotein basigin. The basigin gene is located at p13.3

on chromosome 19 and consists of ten exons spanning 12 kb[18]. Basigin is a member of the immunoglobulin family of cell surface proteins and is expressed as four different isoforms. The transmembrane domain is almost completely conserved across all species, while the cytoplasmic domain is only moderately conserved[19]. The largest isoform, known as basigin-1, has three immunoglobulin domains within the extracellular domain and is expressed specifically in the retina[18]. Basigin-2, also commonly called CD147, is the isoform expressed at relatively high levels in many cell types and possesses two immunoglobulin domains within the extracellular domain. The core protein portion of basigin-2 is 28 kDa[18], and during processing in the cell, it becomes heavily glycosylated on three asparagine residues resulting in an increase in its weight to 43-66 kDa[20]. For the purpose of this thesis, basigin-2 will be referred to as CD147 unless specified otherwise. A study by Jia et al. looked closer at CD147 glycosylation, specifically its interaction with other molecules. Since CD147 associates with caveolin-1 (Cav-1), the authors looked into its effect on glycosylation. Using an RNA interference (RNAi) model, it was shown that downregulation of Cav-1 suppressed the conversion of CD147 into its higher glycosylated form, exhibiting the importance of the CD147/Cav-1 association[21]. Additionally, it was originally thought that CD147 was only able to exhibit stimulatory activity if glycosylated. However, a study by Belton et al. demonstrated that activation is not dependent upon glycosylation of the CD147 ligand[22].

CD147 is normally involved in a number of biological processes including embryonic development, sensory regulation, and immunological responses[18]. While CD147 expression is elevated in rapidly proliferating tumor cells, it is also found in leukocytes, macrophages, epithelial cells (blood vessel walls), red blood cells, and the

endometrium; but not in normal glia[23-24]. A study by Geng et al. found that CD147 promoted M1 macrophage activity in the lungs, which induced the differentiation of cells in lung fibrosis[25]. Another study by Coste et al. examined the function of CD147 in red blood cells. In this study, anti-CD147 monoclonal antibody (mAb) treatment disrupted the circulation of red blood cells, leading to cellular trapping in the spleen[24]. In a study of CD147 deficient mice, the majority of embryos died during implantation. The surviving mutant mice were born underdeveloped and died well before adulthood[26]. In normal mice, CD147 was highly expressed in the embryo proper, endometrium, and trophoblast cells. The early deaths of knockout-CD147 mice suggest its important role in embryogenesis and reproduction[22]. CD147 has also been found to play an important role in the sensory nervous system, as the survival and function of photoreceptors in the retina is dependent upon CD147 through its affiliation with monocarboxylate transporters (MCTs) in the plasma membrane of retinal cells[27]. In the immune system, recent studies have shown that CD147 affects T-cell activation as well as T-cell development[28]. In CD147-knockout mice, thymus development was arrested in early stages[28]. Furthermore, T cell proliferation was significantly increased when CD147 was knocked down using siRNA-mediated gene silencing[29]. Through confocal microscopy, it was found that CD147 is recruited to the immunological synapse during T cell activation[30]. The immunological synapse is the space between the antigen-presenting cell and a lymphocyte. Using a CD147-EGFP (enhanced green fluorescent protein), Ruiz et al. observed that CD147 translocated from the plasma membrane to the immunological synapse upon T cell activation[31].

In cancer cells, CD147 expression levels are significantly higher than in normal tissue. Furthermore, the levels of CD147 expression correlate directly with tumor severity and progression in gliomas and show the highest expression in GBM[32]. In fact, CD147 expression is upregulated in nearly every type of cancer, including breast, cervical, colon, lung, and melanoma among others[33]. In GBM, CD147 promotes tumor growth, inhibits cell death, and enhances the invasiveness of tumor cells[34]. Interactions with many specific proteins are a key part of CD147 function. CD147 acts as an extracellular matrix metalloproteinase (MMP) inducer by stimulating the release of MMPs from fibroblast cells. MMP induction is initiated when a soluble basigin ligand binds to a CD147 cell surface receptor, stimulating the ERK 1/2 signaling pathway which induces expression of MMPs[22]. Matrix metalloproteinases can then degrade the extracellular matrix and therefore assist with tumor invasiveness, angiogenesis, and increased cell survival. CD147 also contributes to angiogenesis independently of MMPs by increasing vascular endothelial growth factor (VEGF), which assists in blood vessel formation as discussed earlier[35]. In a study by Tang et al., VEGF expression was induced in a CD147 dose dependent manner. Furthermore, VEGF expression was inhibited by suppressing CD147 expression in tumor cells by using an anti-CD147 mAb[31]. CD147 has been shown to act as a coreceptor for VEGFR2 in both tumor and endothelial cells. Since CD147 is overexpressed in most cancers, this causes enhanced activation of the VEGFR2 which leads to increased angiogenesis for tumor cells[36].

CD147 also interacts with cell surface transmembrane glycoproteins called integrins, and the association of CD147 with integrins is important for cell adhesion, migration, metastasis, and cell signaling[37]. In CD147 mutant mice, the disruption of this

interaction lead to cellular dysfunction such as abnormal distribution of organelles, including the mitochondria, nuclei, and endoplasmic reticulum[37-38]. In multiple sclerosis, CD147 regulates alpha-4 integrin expression on T cells. A flow cytometry assay showed that T cells treated with an anti-CD147 mAb had reduced alpha-4 integrin expression on the cell surface[39]. While examining the mechanism by which this occurs, Agrawal et al. showed that anti-CD147 mAb treatment inhibited the nuclear factor kB (NFkB) pathway. To test this, the authors examined IκBα protein levels 2 hours post anti-CD147 mAb treatment[39]. IκBα is a protein that functions to inhibit NFkB by interfering with its cell signaling. Western blot analysis demonstrated that when treated with the anti-CD147 mAb, IκBα levels decreased in the cells[39].

Another important protein group that CD147 associates with are cyclophilins, which bind extracellularly and transmit their signals. Cyclophilin A is a peptidylprolyl isomerase normally expressed inside cells but is secreted in response to immunological stimuli such as inflammation and antigen presentation. Secreted cyclophilins promote chemotactic activity for neutrophils, eosinophils, and T cells[18]. Chemotaxis occurs when a cell moves in response to a chemical stimulus. CD147 has been shown to act as a receptor for cyclophilin A and mediate its chemotactic activity towards target cells. This CD147-cyclophilin interaction is important for the inflammatory process of several diseases, including GBM[40]. A recent study by Jin et al. demonstrated that cyclophilin A is secreted by cells in response to oxidative stress[41]. Therapeutic agents that have reduced CD147 expression exhibited a significant anti-inflammatory response, suggesting that the CD147/cyclophilin interaction could be a potential target for anti-inflammatory therapy.

CD147 inhibition through an anti-CD147 mAb reduced inflammation by more than 50% in mouse models with lung inflammation, asthma, and rheumatoid arthritis[40].

CD147 is also indirectly involved in the transport of metabolites such as lactate and pyruvate across the plasma membrane. Monocarboxylate transporters (MCTs) play a central role in this transport, and CD147 forms a complex on the cell surface with these transporters[42]. Walters et al. used immunofluorescence analysis to demonstrate that CD147 specifically interacts with both MCT1 and MCT4 in cancer cells[43]. MCTs are involved in the regulation of glycolytic metabolism, which is crucial for the expansion of neoplastic tissue[44]. Under low oxygen (hypoxic) conditions, glucose is catabolized to lactate through glycolysis to form ATP because the mitochondria can't use oxidative phosphorylation to create ATP without oxygen. Cancer cells can also produce lactate under aerobic conditions – switching from glycolysis and oxidative phosphorylation to strictly cytosolic glycolysis[45]. This phenomenon is called the 'Warburg effect' thanks to its leading contributor, Otto Warburg (figure 1). Lactate, the end product of anaerobic glycolysis, causes acidosis in cells and must be pumped out for cancer cells to remain functional[42]. In a study by Baba et al., blocking expression of the CD147/MCT complex using an anti-CD147 mAb was shown to decrease the number of melanoma and colon cancer cells in vitro through an accumulation of lactate and a decreased pH. Immunofluorescence analysis showed that after mAb treatment, MCT was being internalized into the cell, suggesting internalization of the CD147/MCT complex. This is problematic because the CD147/MCT complex carries out its function on the cell surface. This response was specific for cancer cells, and not for normal fibroblasts[42]. In the study, it is important to note the authors did not detect apoptosis in the anti-CD147 mAb treated

cells, and assumed the decreased cell numbers were caused by necrosis. This is a major assumption because other factors could be causing this, such as an interruption of the cell cycle leading to decreased proliferation.

Eukaryotic cells have two main mechanisms of cell death – apoptosis and necrosis. Apoptosis is a process of enzyme-mediated, programmed cell death whereas necrosis is described as accidental cell death due to environmental stress. The morphology of cells undergoing apoptosis is characterized by cytoplasmic condensation and cellular fragmentation into membrane-bound fragments[46]. Specific proteases called caspases are integral to the apoptotic response. Caspase activation is involved in the production of pro-inflammatory cytokines such as IL-1[47]. Caspase proteolysis of substrates is responsible for the morphological changes in apoptotic cells. Another caspase-dependent process used for apoptosis detection is phosphatidylserine (PS) exposure. In a paper by Martin et al., it was shown that inhibition of specific caspases lead to inhibition of PS externalization.[48]. Molecules called flippases are responsible for keeping PS in the inner leaflet of the plasma membrane, while scramblases are responsible for translocating PS to the outer leaflet[49]. When cells begin apoptosis, PS moves from the inner leaflet to the outer leaflet of the plasma membrane, which exposes it to be detected[46]. The morphology of cells that experience necrotic cell death is significantly different from apoptosis. Necrotic cell death is accompanied by cell swelling, organelle distension, degradation of nuclear DNA, and plasma membrane autophagy[31]. Necrosis is considered to be passive because it requires minimal energy and isn't regulated by any homeostatic mechanism. Necrosis occurs due to several

environmental factors such as nutrient deprivation, reactive oxygen species, toxin exposure, and severe changes in physiological conditions[50].

Aside from cell death, inhibition of signaling pathways can also lead to a decreased number of cells, this time without actually killing them. In a 2014 paper by Huang et al., it was shown that CD147 significantly suppresses p53 protein levels[51]. P53 is a tumor suppressor gene that regulates cellular metabolic stress responses. P53 activity is very low in normal cells, but is increased in response to cellular stress such as DNA damage and oncogene activation[52]. The primary regulator of p53 is mouse double minute 2 homolog (MDM2), which functions to inhibit p53 transcriptional activation. MDM2 does this by acting as a ubiquitin ligase, which induces proteasome degradation to decrease p53 protein levels[52]. Many studies have shown that p53 inhibits the expression of glucose transporters GLUT1 and GLUT4, which are both crucial for energy production[51]. P53 is downstream of the PI3K/Akt/MDM2 signal transduction pathway, which is critical in cellular functions such as proliferation, glucose metabolism, and angiogenesis (figure 2). Specific growth factors lead to activation of this pathway and one of these key regulators is epidermal growth factor (EGF) and its receptor EGFR. EGFR lays directly upstream of the PI3K/Akt/MDM2 pathway and its activation leads to activation of the pathway[53]. EGFR is a receptor tyrosine kinase (RTK) that is upregulated in several types of cancers including breast cancer, pancreatic cancer, and GBM[53]. To become activated, RTKs generally require ligand binding that eventually leads to phosphorylation of the receptor. Interestingly enough, in cancer, RTKs can become phosphorylated in the absence of a ligand. Overexpression or mutations of RTKs can lead to clustering of receptors, causing them to homodimerize and become phosphorylated

without a ligand[54]. Interestingly enough, EGFR variant 3 (EGFRvIII), which is a ligand-independent receptor, is overexpressed in GBM[55]. EGFR is known for its role in cell proliferation and inhibition of apoptosis, which is why it is labeled as a proto-oncogene. A proto-oncogene is a normal gene that has potential to become mutated and eventually cause cancer. In a paper by Grass et al, it was demonstrated that CD147 forms a complex with EGFR in lipid-raft membrane domains[56]. To test this, a proximity ligation assay (PLA) that examines the association of specific proteins was conducted. The assay demonstrated that there is close association between CD147 and EGFR inside membrane fractions of cancer cells[56]. Given that CD147 is also directly upstream of the PI3K/Akt/MDM2 signaling pathway, it was hypothesized by Huang et al. that CD147-activated Akt may lead to the degradation of p53. Upon further analysis, it was found that phosphorylation of Akt and MDM2 was significantly decreased when CD147 was either knocked down or knocked out, all while p53 levels increased. These results suggest that CD147 may activate the PI3K/Akt/MDM2 pathway to inhibit p53 by promoting its degradation[51]. Furthermore, the study demonstrated an inverse correlation between lactic acidosis and PI3K/Akt activity. Huang et al. found that Akt activity was reduced by a MCT1 specific siRNA or a MCT1 inhibitor, while it was significantly increased in MCT1 overexpressing cells[51]. Taken together, this data suggests that the CD147/MCT complex along with EGFR activity play a role in activating the PI3K/Akt/MDM2 pathway. To conclude, inhibiting CD147 may subsequently inhibit the PI3K/Akt/MDM2 pathway, leading to increased p53 expression and its tumor suppressing properties.

In the human body, cells are either surrounded by the extracellular matrix or are in direct contact with other cells. However, most in vitro biology techniques culture cells

in a two-dimensional (2D) monolayer on plastic, which isn't representative of a cells natural microenvironment[57]. In an attempt to mimic the body as accurately as possible, three-dimensional (3D) cell culturing techniques have recently been developed. In the thesis presented here, an improved cell culturing technique was developed to culture multi-cellular 3D spheroids using ultra-low attachment 96-well plates. Three-dimensional growth of cells is now regarded as a more reliable model in comparison to single adherent cells when conducting cell culture assays. Spheroids possess several similar features of tumors such as cell interactions, response, and resistance[58]. Improvements of several other physiological aspects have also been highlighted using 3D cell culture, such as – cell viability, morphology, proliferation, differentiation, invasion, angiogenesis, and cell function[59]. The 3D spheroid model more closely imitates in vivo cells, with the expectation that it will give the most accurate and reliable results. In the work discussed below, we used a 3D cell culture system and anti-CD147 mAbs to test whether CD147 could be targeted for anti-tumor therapy.

AIMS AND GOALS

Glioblastoma (GBM) is the most common and lethal form of primary cancer in the central nervous system. While normal glial cells do not express CD147, the transmembrane glycoprotein is highly overexpressed in GBM. CD147 contributes to critical tumor promoting properties, which eventually lead to increased tumor cell survival. This presents an important target for a potential therapeutic treatment. CD147 forms a complex with monocarboxylate transporters (MCTs) on the cell surface, which serves as an important regulator of intracellular homeostasis. Activation of this complex may lead to activation of the PI3K/Akt/MDM2 pathway, which subsequently inhibits p53, an important tumor suppressing protein. A 2008 paper by Baba et al. showed that blocking formation of the CD147/MCT complex using an anti-CD147 mAb decreased the number of melanoma and colon cancer cells through an accumulation of lactate and a decreased pH[42]. This decreased cell number was exhibited in cancer cells, but not in normal fibroblasts[42].

Our hypothesis was that treating U87MG GBM cells with anti-CD147 mAbs would suppress tumor cell growth in a multi-cellular tumor spheroid model. To test this hypothesis, U87MG GBM multi-cellular tumor spheroids were grown in 96-well ultra-low attachment round bottom plates, and treated with anti-CD147 mAbs. During mAb treatment, spheroids were measured every 24 hours and compared to controls. The

possible mechanism by which the mAbs suppressed cell growth was tested to determine if the effects were a result of cell death or cellular proliferation.

METHODS AND MATERIALS

Cell Culture

U87MG adherent cells (ATCC) were cultured in Eagle's Modified Essential Medium (EMEM; Corning, Manassas, VA) with 10% Fetal Bovine Serum (FBS; Atlanta Biological, Atlanta, GA). The media was supplemented with 1% Penicillin-Streptomycin-Amphotericin B (PSA; Lonza, Walkersville, MD) to prevent bacterial and fungal contamination. Under laminar flow, frozen aliquots of cells were resuspended in 8.5 ml of culture media and then transferred to 75cm^2 tissue treated flasks. Each flask was incubated at 37ºC and 5% CO_2 until cells became nearly confluent, where cells were then either passaged 1:3, harvested for replating or for spheroid assays.

Spheroid Antibody Assay

Once nearly confluent, cells were removed from the flask with trypsin-versene (Lonza) and pelleted at 1000 rpm for 5 minutes. Pelleted cells were resuspended in 10 ml culture medium, and the live cells were counted using a hemacytometer (Hausser Scientific, Horsham, PA) following trypan blue solution staining of the cells (VWR Life Science AMRESCO, Radnor, PA). 96-well round bottom ultra low attachment plates (Corning) were used for the growth of spheroids. Cells were plated at 500 cells/well in 100 μl of culture media. Immediately after cell plating, an additional 100 μl of either antibody-treated media, or normal culture media was added to each well. Three different

anti-CD147 monoclonal antibodies (mAbs) were used throughout the duration of these assays – Ab666 (Abcam, Cambridge, MA), MEM-M6/1 (Genetex, Irvine, CA), and P2C2 (Dr. Robert Belton, University of Illinois). Antibody treatment consisted of two different concentrations for each mAb – 2 μg/ml, and 10 μg/ml. Seven wells were used for each treatment condition. Spheroid cultures in the 96-well plate were placed into incubation and analyzed for growth at 24-hour time points for 7 days. Spheroids were measured using an ocular micrometer attached to a Microscoptics IV900 series microscope. A Canon EOS Rebel T6 camera attached to the microscope was used to photograph each spheroid at 24-hour time points.

Apoptosis/Necrosis Detection Assay (Abcam)

24-well tissue treated plates (Corning) were used for cell culture. 12mm poly-d lysine coated coverslips (Corning) were placed at the bottom of each well to be used for fluorescent microscopy upon assay completion. Cells were plated at 20,000 cells/well in 500ml of culture media. Immediately after cell plating, an additional 500ml of either antibody-treated media, or normal culture media was added to each well. Anti-CD147 mAb ab666 was used at a concentration of 10 μg/ml for each treatment well. Cells were then placed into incubation and grown for 4 days. After day 4, prior to beginning the apoptosis/necrosis detection kit, positive control cells were treated with 1 μm staurosporine for 3.5 hours to induce cell death. All cells were then washed 2 times with 500 μl assay buffer, by carefully pipetting the buffer up and down. Next, cells were resuspended in 600 μl assay buffer and treated with 6 μl 100X apopxin deep red indicator, 3 μl 200X nuclear green, and 3 μl 200X cytocalcein 450 in order to measure the presence of apoptotic or necrotic events. Cells were then incubated at room

temperature for 45 minutes. After incubation, cells were washed with 500 μl assay buffer then resuspended in 500 μl assay buffer. Finally, cells were imaged using cellSens software and an Olympus DP72 fluorescent microscope.

CellQuanti-Blue Proliferation Assay (BioAssay Systems)

Living cells actively reduce the CellQuanti-Blue solution and convert it into a highly fluorescent product. The measured fluorescent activity directly correlates with a cells metabolic activity, which provides a relatively easy way to measure cell proliferation. For this assay, cells were plated at 5,000 cells/well in 50 μl of culture media. Black 96-well clear bottom plates (Corning) were used for cell culture. Immediately after cell plating, an additional 50 μl of either antibody-treated media, or normal culture media was added to each well. Anti-CD147 mAb ab666 was used at a concentration of 10 μg/ml for each treatment well. Cells were then placed into incubation and grown for 4 days. After day 4, CellQuanti-Blue reagent was equilibrated to room temp then added to each well at a volume of 10 μl. Cells were then incubated at room temperature for 2 hours and subsequently analyzed on a Modulus microplate multimode reader (Turner Biosystems, Sunnyvale, CA) using a 530 excitation/590 emission filter.

Statistical Analysis

Spheroid size was averaged for each culture condition and plotted for daily change in growth in Microsoft excel. Data from each antibody concentration was analyzed against the control in a paired t-test for each day using GraphPad. Data with a P value <0.05 was considered significant. Data with a P value <0.01 was considered highly significant. Data with a P value <0.001 was considered extremely significant. For apoptosis/necrosis detection, a cell count was done for each stain to determine percent

change between control and treated samples. Data from the CellQuanti-Blue proliferation assay was calculated as percent change in cell number of treated cells compared with controls. Data with a P value <0.05 was considered significant. Data with a P value <0.01 was considered highly significant. Data with a P value <0.001 was considered the most significant.

RESULTS

Spheroid Growth

Because the literature indicates that CD147 interference/knockdown leads to decreased tumor cell survival, it was hypothesized that anti-CD147 mAbs would inhibit CD147 function and therefore suppress spheroid growth. Prior to setting up the spheroid antibody assay, it was first demonstrated that U87MG cells could form spheroids. Initially, two different types of spheroid plates were used. Plates treated with poly-HEMA and plates treated with agarose were both initially tested. Both substances were used because of their relatively low prices and their ability to produce hydrophobic surfaces in the culture dish, which favor spheroid growth. Spheroids were able to form in both plates, but the bottom of the plates contained so much amorphous material that images were distorted, making spheroid measurements impossible. To correct this, ultra-low attachment plates were purchased from Corning and used for the remainder of the study. U87MG cells formed spheroids in these low-attachment plates and allowed for clear images.

Spheroid Antibody Assay

Initially, to assure spheroids would grow in the presence of mAbs, 500 U87MG cells were plated along with anti-CD147 mAb ab666 at a concentration of 10 μg/ml. After incubating overnight, spheroids formed and therefore allowed for the spheroid

antibody assay to begin. The spheroid assay was done in three different trials, with seven different spheroids grown in each each row for every trial (figure 3). In trial 1, five rows were tested. For row A, U87MG cells were plated at 500 cells/well and then treated with standard culture media for a final volume of 200 μl. Cells were grown for 7 days and measured at 24-hour time points (figures 4-6). For rows B and C, U87MG cells were plated at 500 cells/well and then treated with anti-CD147 mAb ab666 at concentrations of 2 μg/ml and 10 μg/ml, respectively. Spheroids were grown for 7 days and measured at 24-hour time points (figures 7-9). For rows D and E, U87MG cells were plated at 500 cells/well and then treated with anti-CD147 mAb P2C2 at concentrations of 2 μg/ml and 10 μg/ml, respectively. Spheroids were grown for 7 days and measured at 24-hour time points (figures 10-12). For trials 2 and 3, a 2nd clone of anti-CD147 mAb MEM-M6/1 was acquired and used throughout the assays. Trials 2 and 3 now had 7 rows in comparison to 5 rows in trial 1. Rows A-E remained the same as trial 1, while 2 new culture conditions were added. For rows F and G, U87MG cells were plated at 500 cells/well and then treated with anti-CD147 mAb MEM-M6/1 at concentrations of 2 μg/ml and 10 μg/ml, respectively. Spheroids were grown for 7 days and measured at 24-hour time points (figures 13-15).

Data for all 3 mabs was averaged and graphed using Microsoft Excel (figures 16-18). Anti-CD147 mab ab666 significantly suppressed spheroid growth on all days after day 1 at a concentration of 10 μg/ml. Growth was suppressed up to 24 percent of the control. Anti-CD147 mab P2C2 significantly suppressed spheroid growth on all days after day 1 at a concentration of 10 μg/ml. Growth was suppressed up to 11 percent of the control. Anti-CD147 mab MEM-M6/1 significantly suppressed spheroid growth on all

days after day 1 at a concentration of 10 μg/ml. Growth was suppressed up to 32 percent of the control. Taken together, it can be said with confidence that CD147 interference through the use of anti-CD147 mAbs significantly suppressed cell growth.

Apoptosis/Necrosis Assay

In order to determine the possible mechanism(s) for anti-CD147 mAb inhibition of spheroid growth, a cell death assay was performed. Instead of 96-well plates, 24-well plates were used and seeded at a higher density. Well 1 was used as the positive control. U87MG cells were plated at 20,000 cells and treated wih standard culture media. After growing for 4 days, cells were treated with 1 μm staurosporine for 3.5 hours to induce cell death and then imaged on a flurouescence microscope (figures 19-22). Figure 19 shows live cells, stained with CytoCalcein Violet 450. Figure 20 shows the same culture stained for apoptotic cells using the Apopxin Deep Red Indicator. Figure 21 shows necrotic cells, stained with Nuclear Green DSC1. Figure 22 shows the overlay image of the 3 stains. 3.5 hours of 1 μm staurosporine successfully induced cell death in the U87MG cells, demonstrating positive staining for both apoptosis and necrosis. Well 2 was used as the negative control. U87MG cells were plated at 20,000 cells and treated with standard culture media. Cells were grown for 4 days and then imaged on a fluroecence microscope (figures 23-26). Figure 23 shows live cells, stained with CytoCalcein 450. Figures 24 and 25 were stained for apoptosis and necrosis respectively. The results are negative for both stains, meaning that the negative control cells did not undergo either mechanism of cell death as a result of the culturing procedures used. Figure 26 shows the overlay image for all 3 stains. Well 3 was the anti-CD147 mAb treated cells. U87MG cells were plated at 20,000 cells and treated with anti-CD147 mAb

ab666 at a concentration of 10 μg/ml. Cells were grown for 4 days and then imaged on a fluorescence microscope (figures 27-39). Figure 27 shows live cells, stained with CytoCalcein 450. Figures 28 and 29 were stained for apoptosis and necrosis respectively. The results were negative for both stains, meaning that the anti-CD147 mAb treated cells are not experiencing any mechanism of cell death. Figure 30 is the overlay image of all 3 stains. All 3 conditions were graphed using Microsoft Excel (figure 31) and expressed as a percent change between control and treated samples. The positive control cells showed significant amounts of both mechanisms of cell death while the negative control and mAb treated cells showed no form of cell death.

CellQuanti-Blue Proliferation Assay

The CellQuanti-Blue proliferation assay followed a similar protocol as previous assays. U87MG cells were plated into a 96-well plate at 5,000 cells/well and treated with anti-CD147 mAb ab666 at a concentration of 10 μg/ml, or left untreated. After 4 days of growth, cells were treated with 10 μl of Cell-Quanti Blue reagent and incubated for 1 hour. Fluorescent intensity was then measured for each well on a fluorescent microplate reader using the 530 excitation/590 emission filter. Graphpad was used to create the graph (figure 32) of cell proliferation. Data was expressed as a percent change between treated and control samples. Ab666 mAb treatment significantly decreased cell proliferation when compared to untreated control cells. A paired t test presented a value of 0.005, confirming significance of the data.

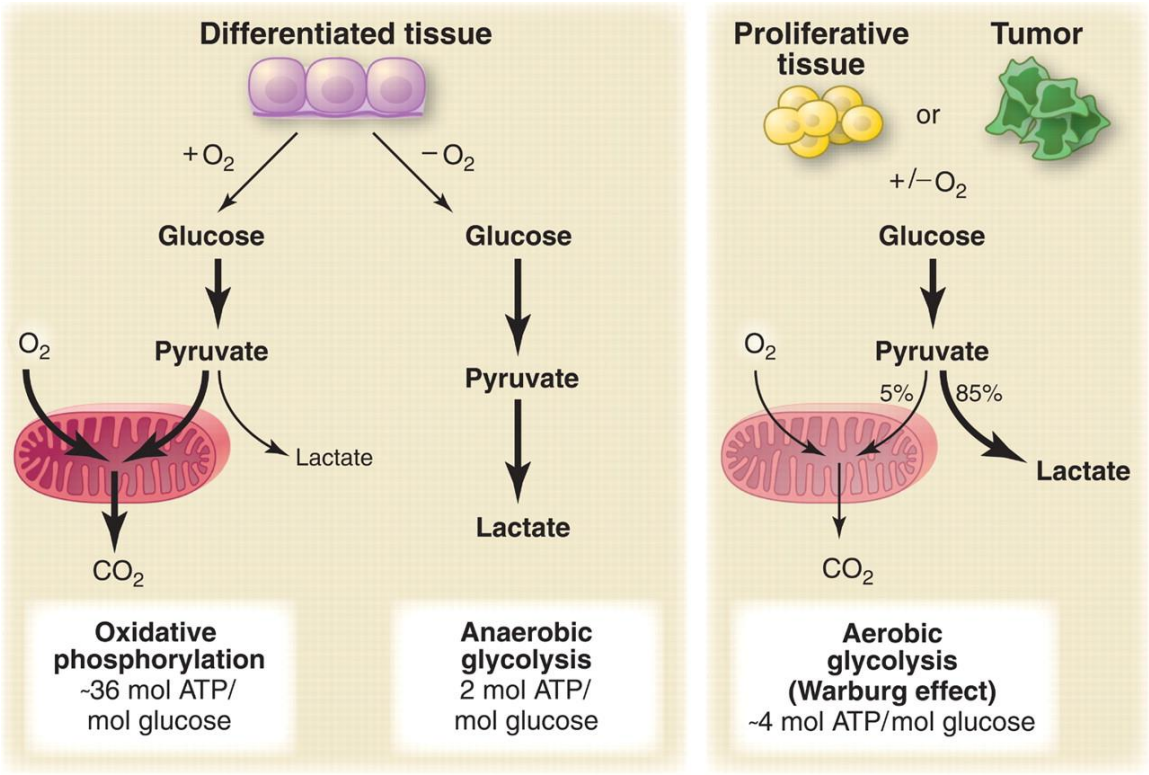

Figure 1: The Warburg effect. In the presence of oxygen, normal cells produce their energy through oxidative phosphorylation. In the absence of oxygen, cells will produce energy through anaerobic glycolysis. Cancer cells produce the majority of their energy, even in the presence of oxygen, though aerobic glycolysis followed by lactic acid fermentation. This is called the Warburg effect. Taken from "Understanding the Warburg effect: the metabolic requirements of cell proliferation" by Heiden et al., 2009, *Science*, Vol. 324, pg. 1029-1033. Used with permission.

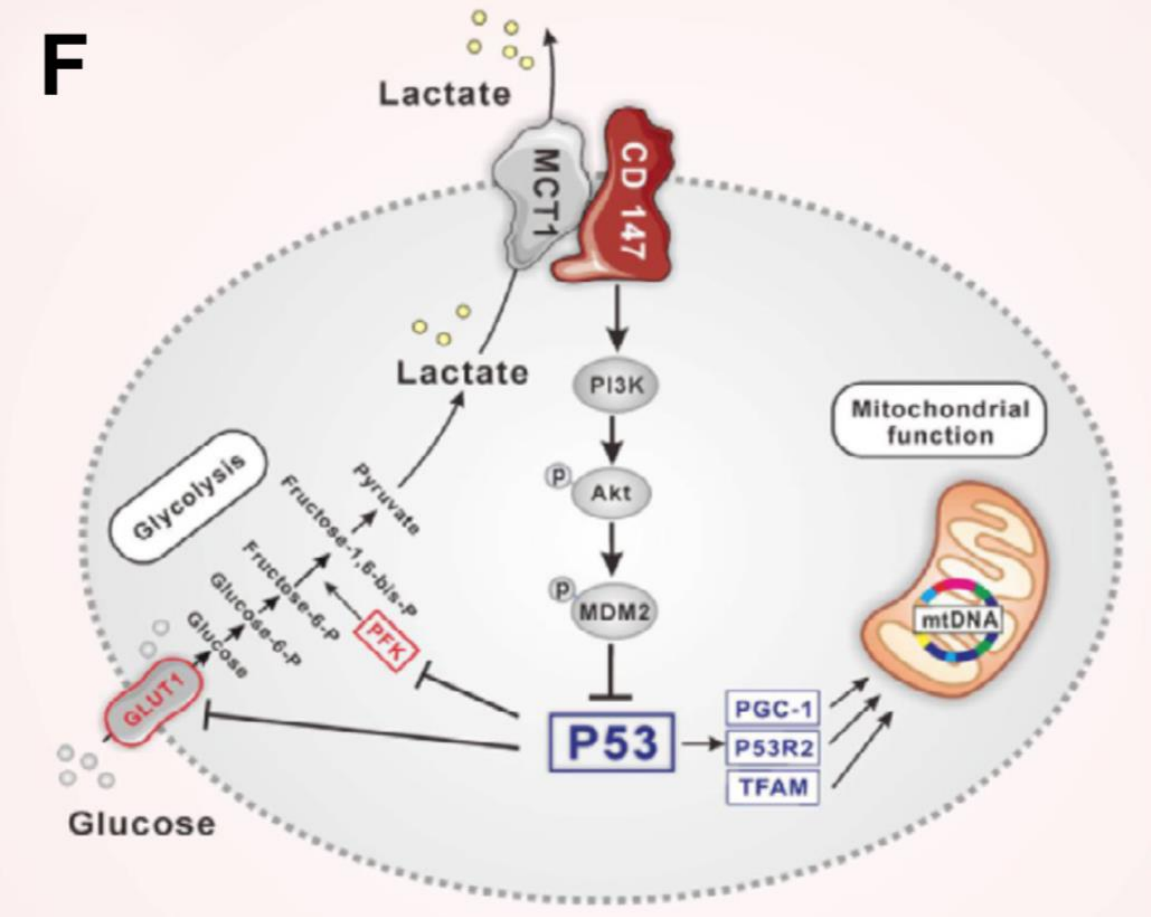

Figure 2: PI3K/Akt/MDM2 pathway. CD147 stimulates the PI3K/Akt/MDM2 pathway. Activation of this pathway leads to the inhibition of p53, a tumor suppressor genes involved in the cell cycle. CD147 inhibition leads to inhibition of the PI3K/Akt/MDM2 pathway, and therefore removes the p53 blockade, allowing it to perform its proper function. Taken from "CD147 promotes reprogramming of glucose metabolism and cell proliferation in HCC cells by inhibiting the p53-dependent signaling pathway" by Huang et al., 2014, *Journal of Hepatology,* Vol. 4, pg. 859-866. Used with permission.

Spheroid Antibody Assay Experimental Design

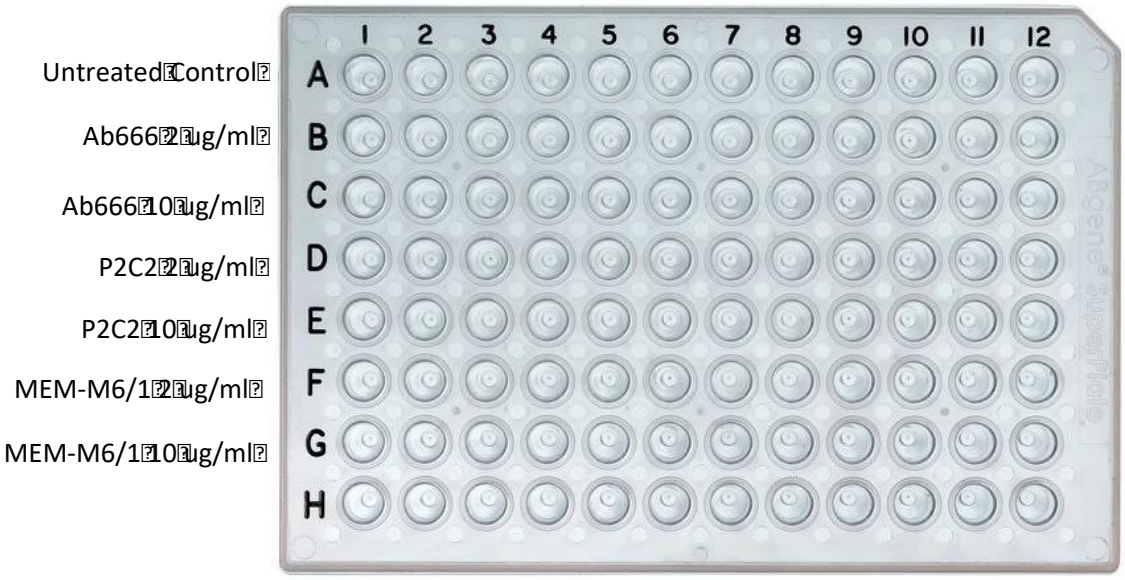

*MEM-M6/1 not used in trial 1

Figure 3: Spheroid antibody assay experimental design. Row A contains the untreated control. Row B contains ab666 at a concentration of 2 ug/ml. Row C contains ab666 at a concentration of 10 ug/ml. Row D contains P2C2 at a concentration of 2 ug/ml. Row E contains P2C2 at a concentration of 10 ug/ml. Row F contains MEM-M6/1 at a concentration of 2 ug/ml. Row G contains MEM-M6/1 at a concentration of 10 ug/ml. MEM-M6/1 was only used in trials 2 and 3.

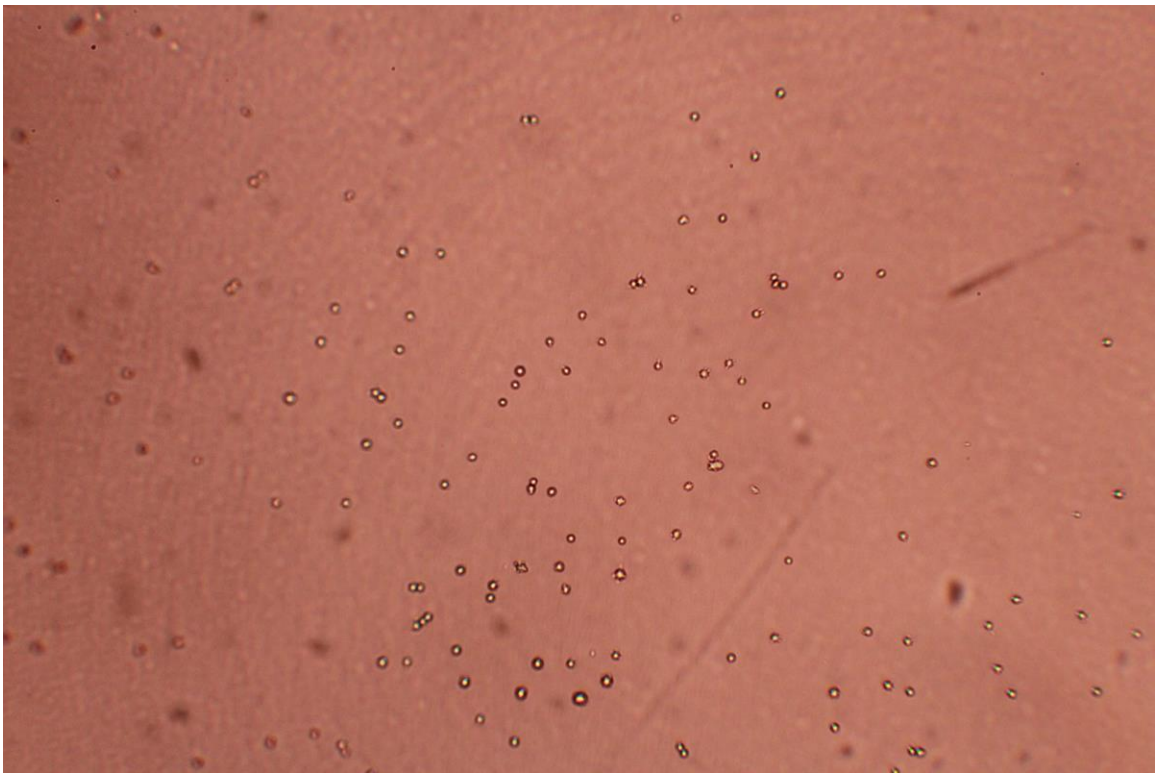

Figure 4: Untreated U87MG cells – day 0. U87MG cells were plated at 500 cells/well. Picture was taken at 4x magnification immediately after cell plating on day 0.

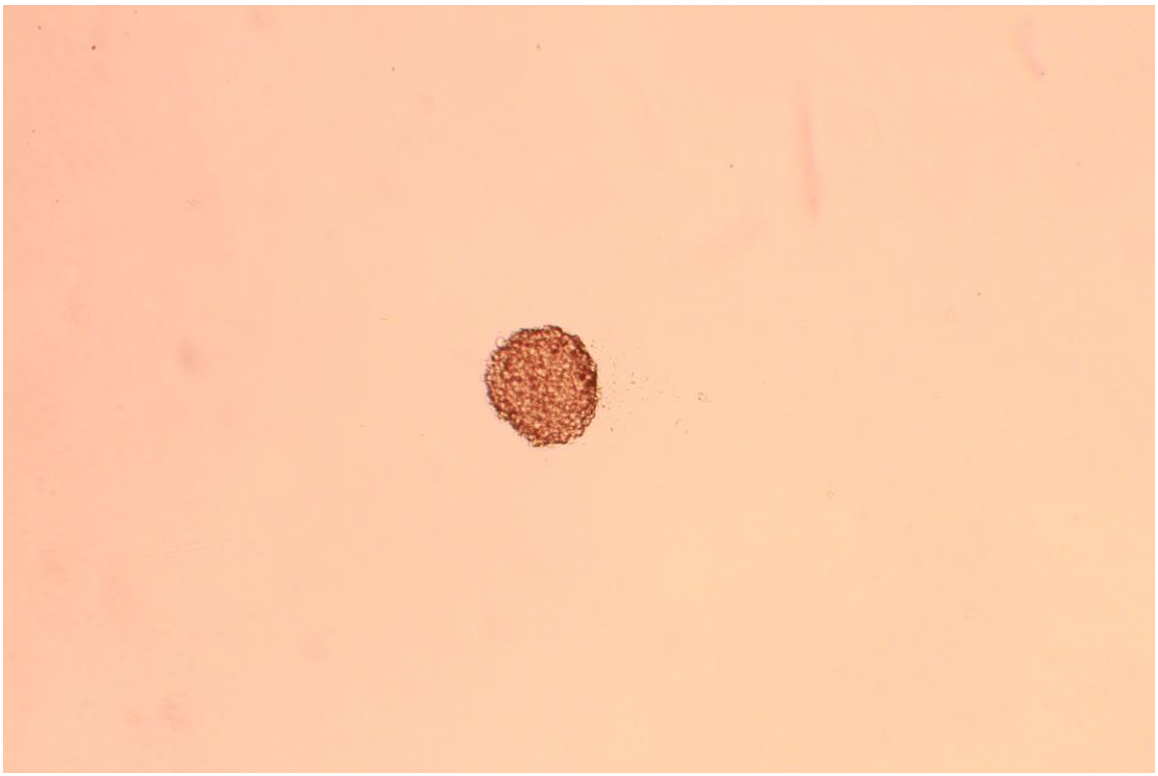

Figure 5: Untreated spheroid – day 3. Control well. Cells were plated at 500 cells/well. Picture was taken at 4x magnification after 72 hours of growth on day 3. Spheroid is 300 micrometers. Measurements were taken using an ocular micrometer and converted using the 4x magnification scale.

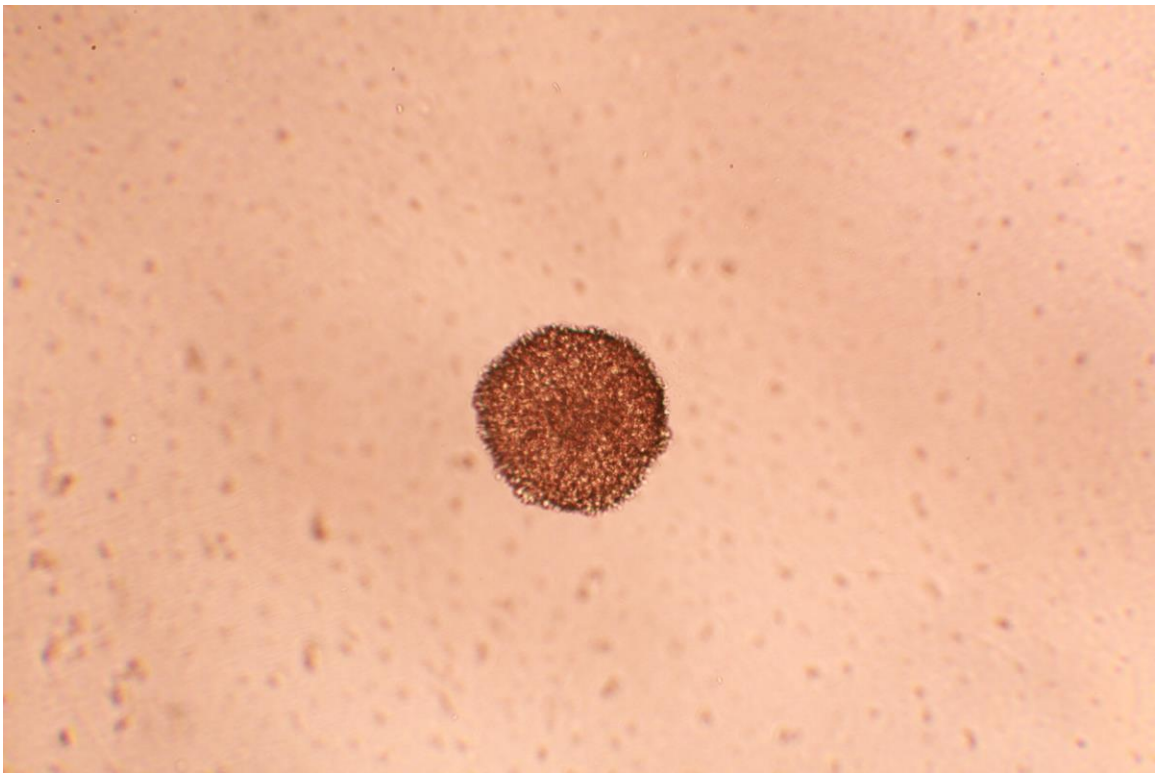

Figure 6: Untreated spheroid – day 6. Control well. Cells were plated at 500 cells per well. Picture was taken at 4x magnification after 144 hours of growth on day 6. Spheroid is 475 micrometers. Measurements were taken using an ocular micrometer and converted using the 4x magnification scale.

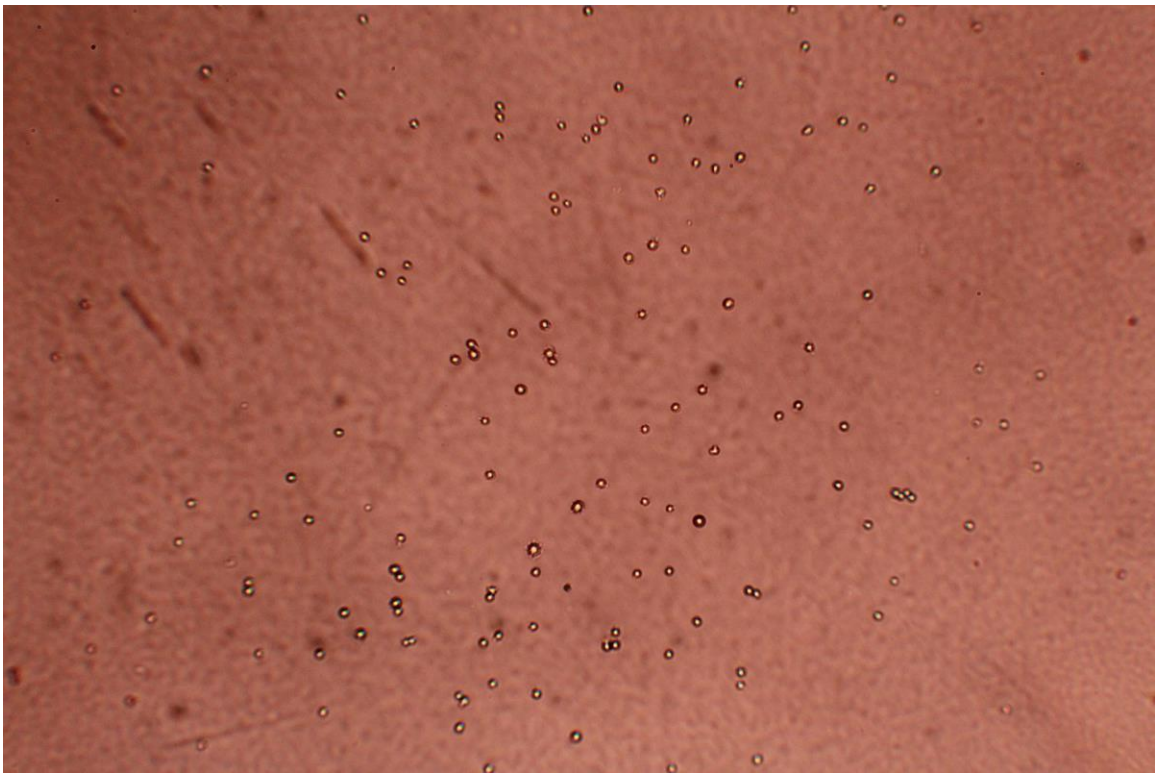

Figure 7: U87MG cells treated with mAb ab666 at 10 μg/ml – day 0. Cells were plated at 500 cells per well and treated with anti-CD147 mAb ab666 at a concentration of 10 μg/ml. Picture was taken at 4x magnification immediately after cell plating on day 0.

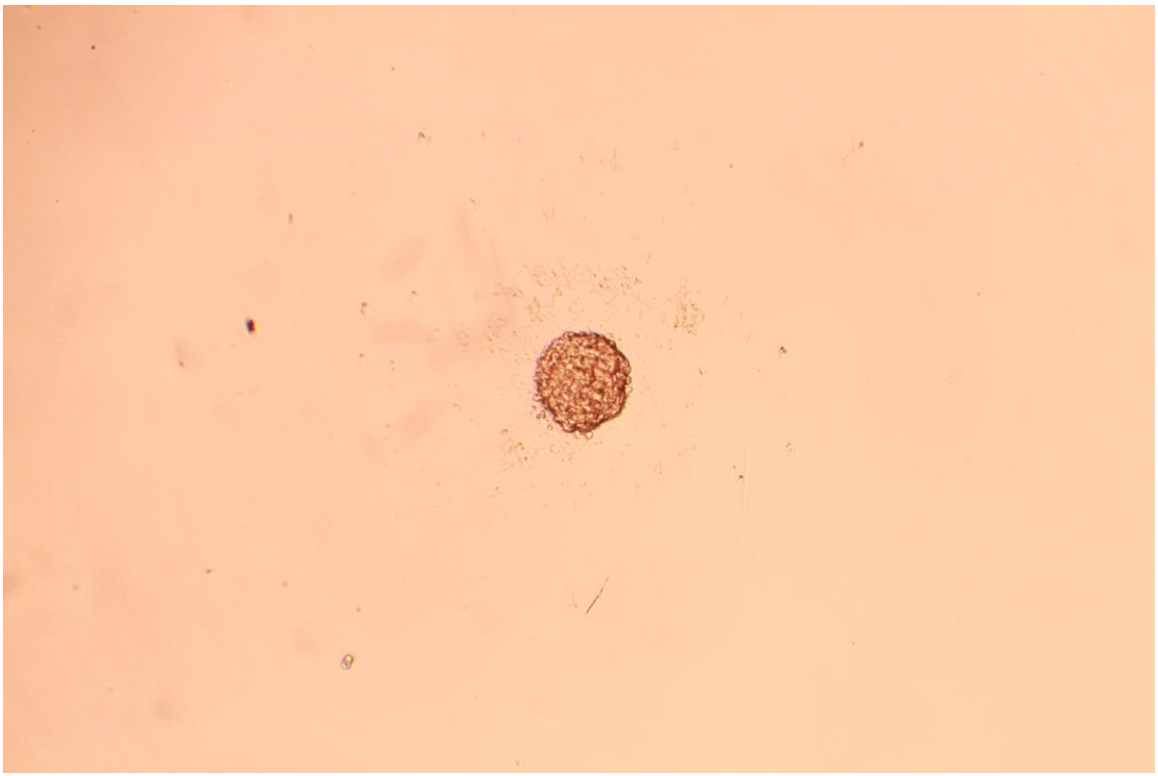

Figure 8: Spheroid treated with mAb ab666 at 10 µg/ml – day 3. Cells were plated at 500 cells per well and treated with anti-CD147 mAb ab666 at a concentration of 10 µg/ml. Picture was taken at 4x magnification after 72 hours of growth on day 3. Spheroid is 225 micrometers. Measurements were taken using an ocular micrometer and converted using the 4x magnification scale.

Figure 9: Spheroid treated with mAb ab666 at 10 μg/ml – day 6. Cells were plated at 500 cells per well and treated with anti-CD147 mAb ab666 at a concentration of 10 μg/ml. Picture was taken at 4x magnification after 144 hours of growth on day 6. Spheroid is 375 micrometers. Measurements were taken using an ocular micrometer and converted using the 4x magnification scale.

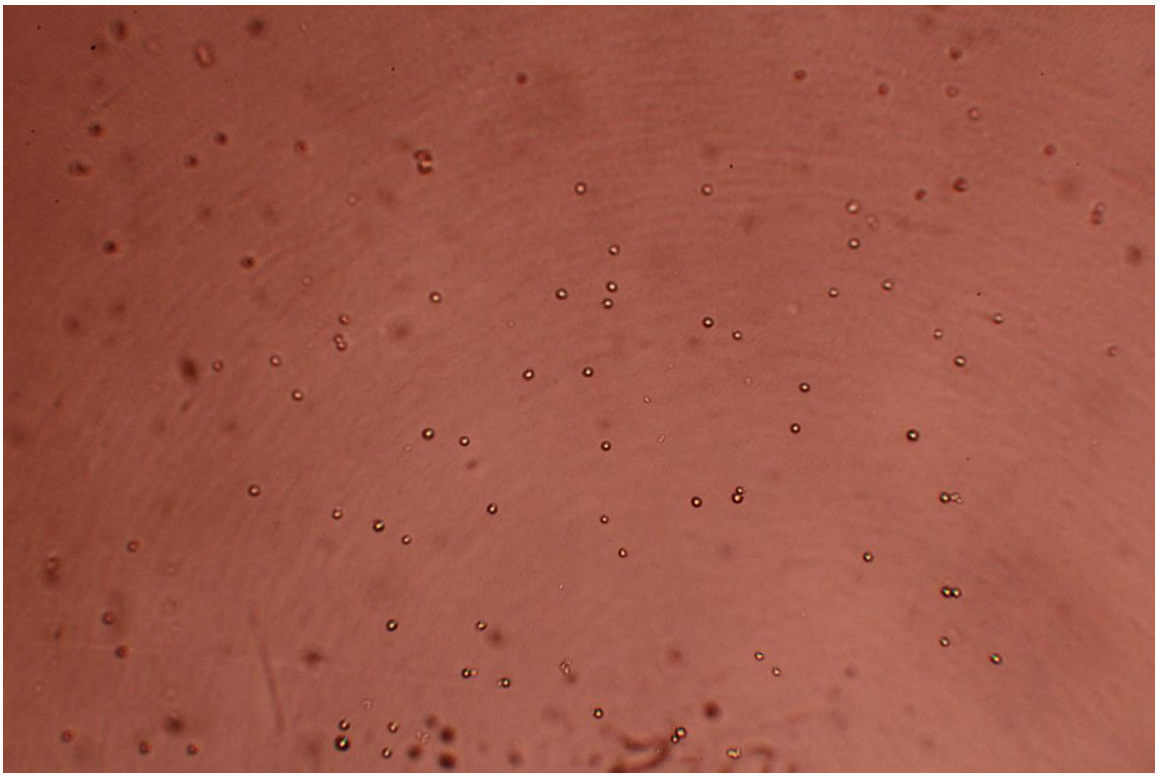

Figure 10: U87MG cells treated with mAb P2C2 at 10 μg/ml – day 0. Cells were plated at 500 cells per well and treated with anti-CD147 mAb P2C2 at a concentration of 10 μg/ml. Picture was taken at 4x magnification immediately after cell plating on day 0.

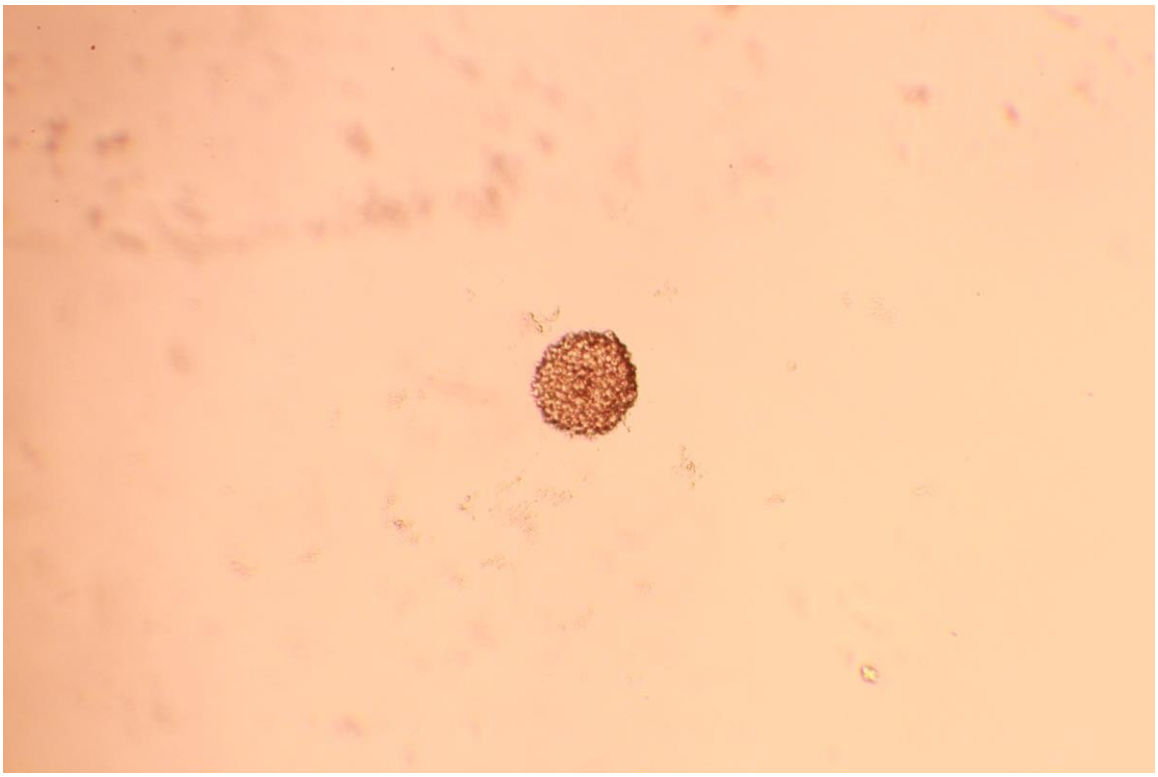

Figure 11: Spheroid treated with mAb P2C2 at 10 μg/ml – day 3. Cells were plated at 500 cells per well and treated with anti-CD147 mAb P2C2 at a concentration of 10 μg/ml. Picture was taken at 4x magnification after 72 hours of growth on day 3. Spheroid is 275 micrometers. Measurements were taken using an ocular micrometer and converted using the 4x magnification scale.

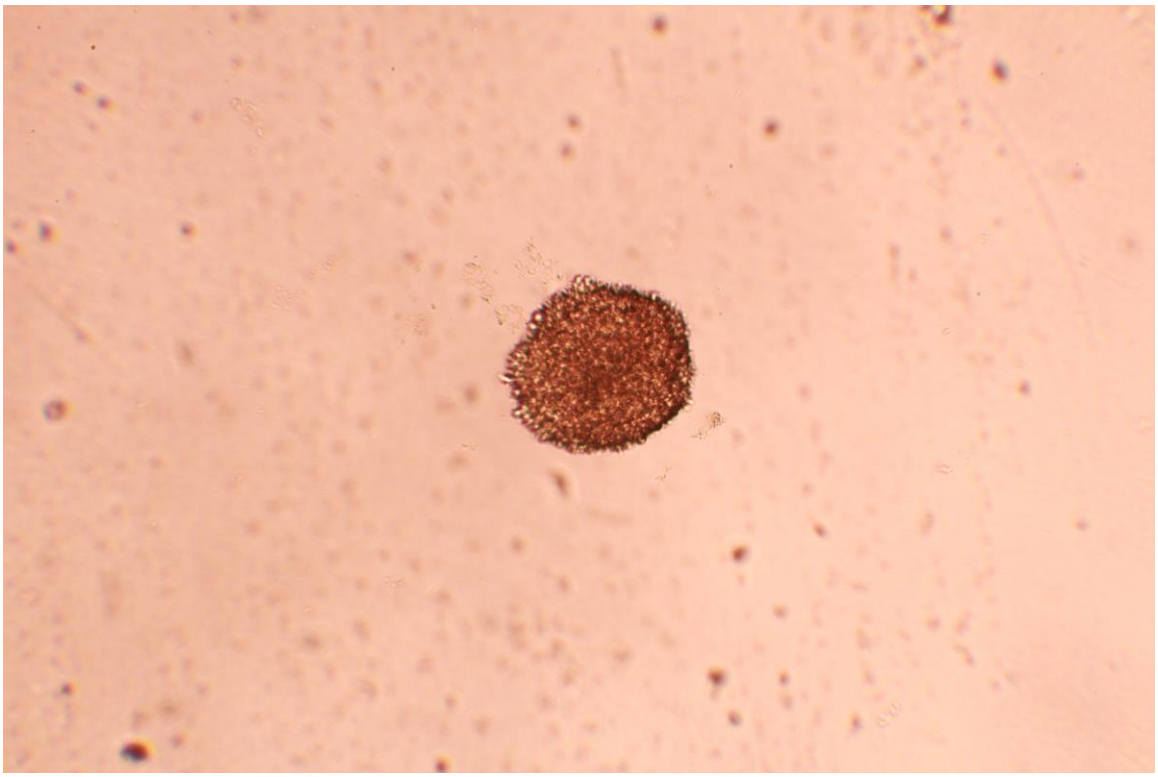

Figure 12: Spheroid treated with mAb P2C2 at 10 μg/ml – day 6. Cells were plated at 500 cells per well and treated with anti-CD147 mAb P2C2 at a concentration of 10 μg/ml. Picture was taken at 4x magnification after 144 hours of growth on day 6. Spheroid is 425 micrometers. Measurements were taken using an ocular micrometer and converted using the 4x magnification scale.

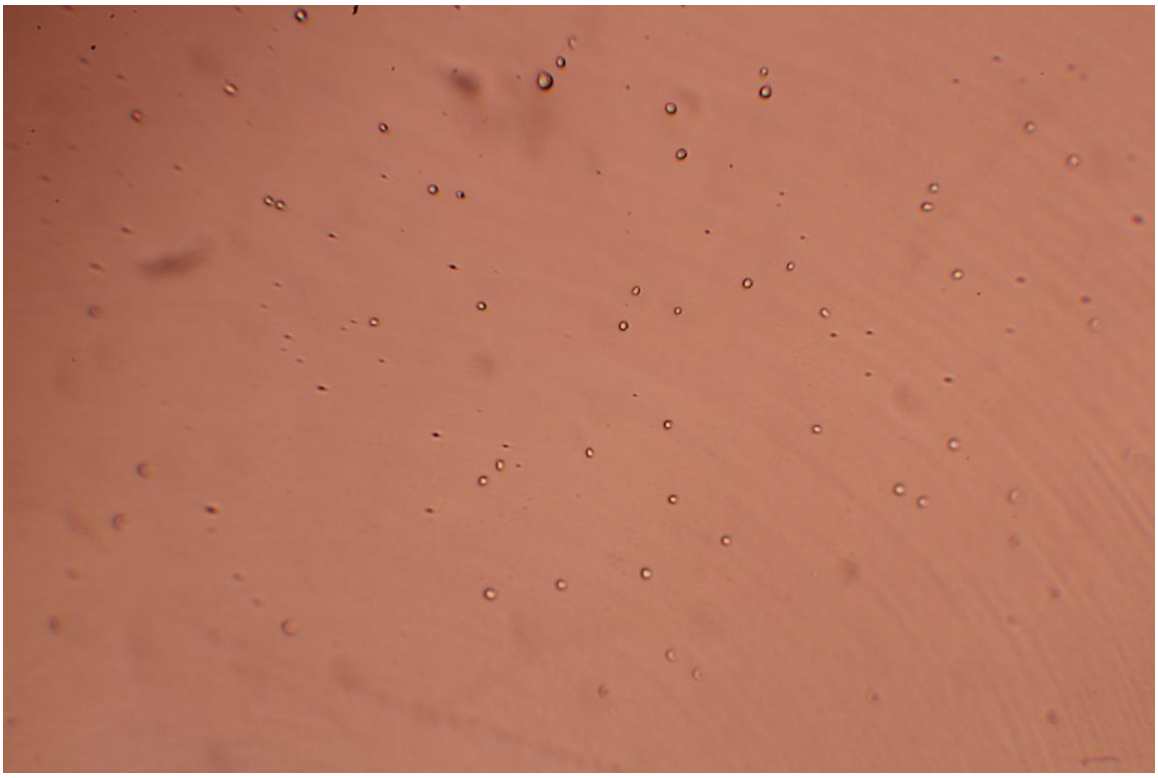

Figure 13: U87MG cells treated with mAb MEM-M6/1 at 10 μg/ml – day 0. Cells were plated at 500 cells per well and treated with anti-CD147 mAb MEM-M6/1 at a concentration of 10 μg/ml. Picture was taken at 4x magnification immediately after cell plating on day 0.

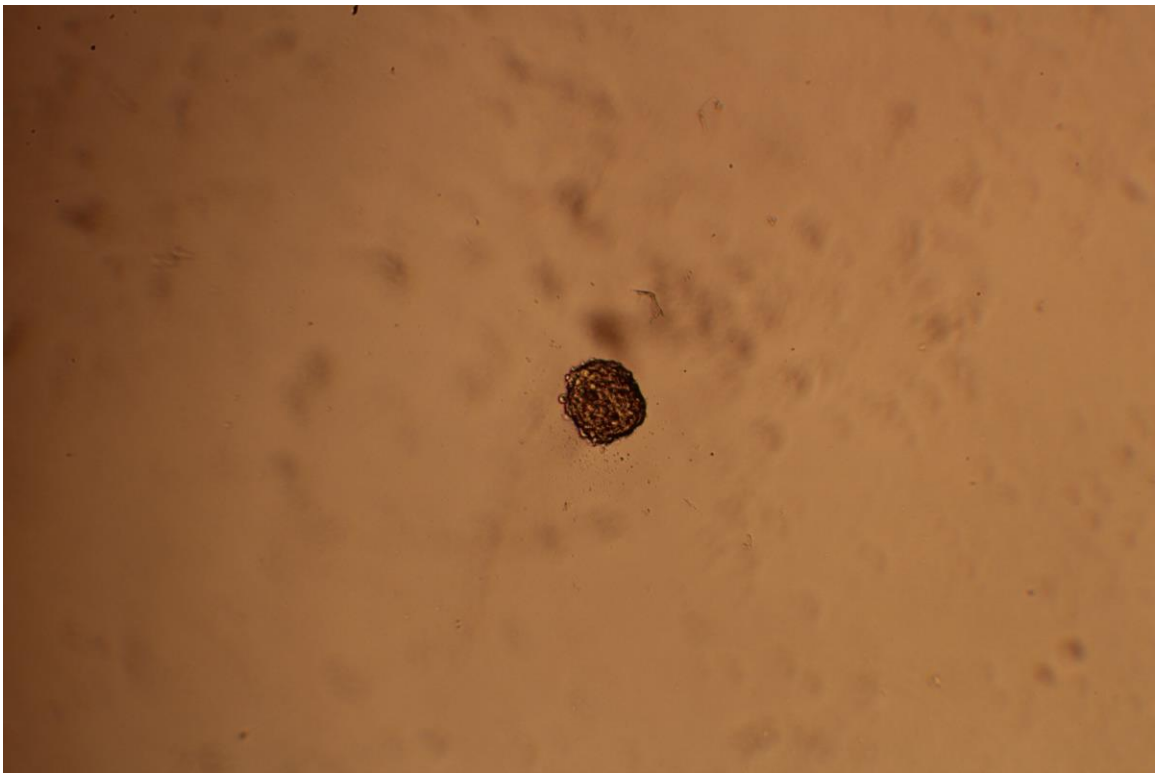

Figure 14: Spheroid treated with mAb MEM-M6/1 at 10 μg/ml – day 3. Cells were plated at 500 cells per well and treated with anti-CD147 mAb MEM-M6/1 at a concentration of 10 μg/ml. Picture was taken at 4x magnification after 72 hours of growth on day 3. Spheroid is 200 micrometers. Measurements were taken using an ocular micrometer and converted using the 4x magnification scale.

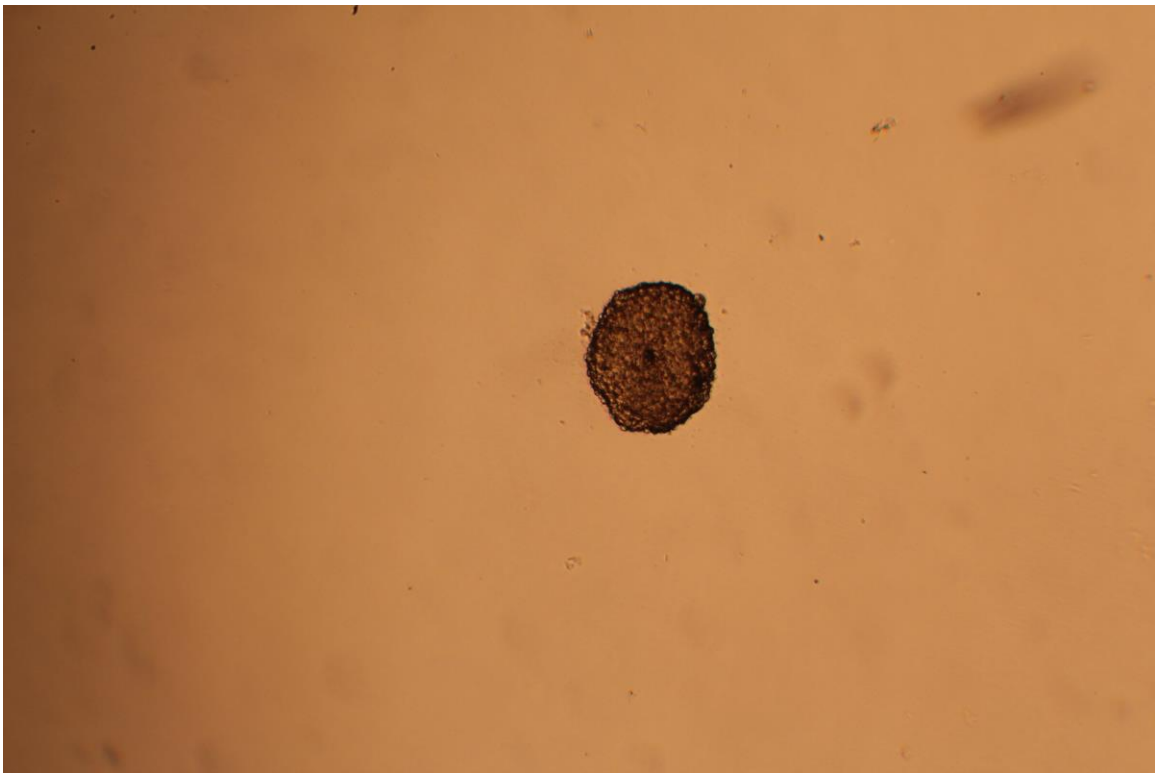

Figure 15: Spheroid treated with mAb MEM-M6/1 at 10 μg/ml – day 6. Cells were plated at 500 cells per well and treated with anti-CD147 mAb MEM-M6/1 at a concentration of 10 μg/ml. Picture was taken at 4x magnification after 144 hours of growth on day 6. Spheroid is 325 micrometers. Measurements were taken using an ocular micrometer and converted using the 4x magnification scale.

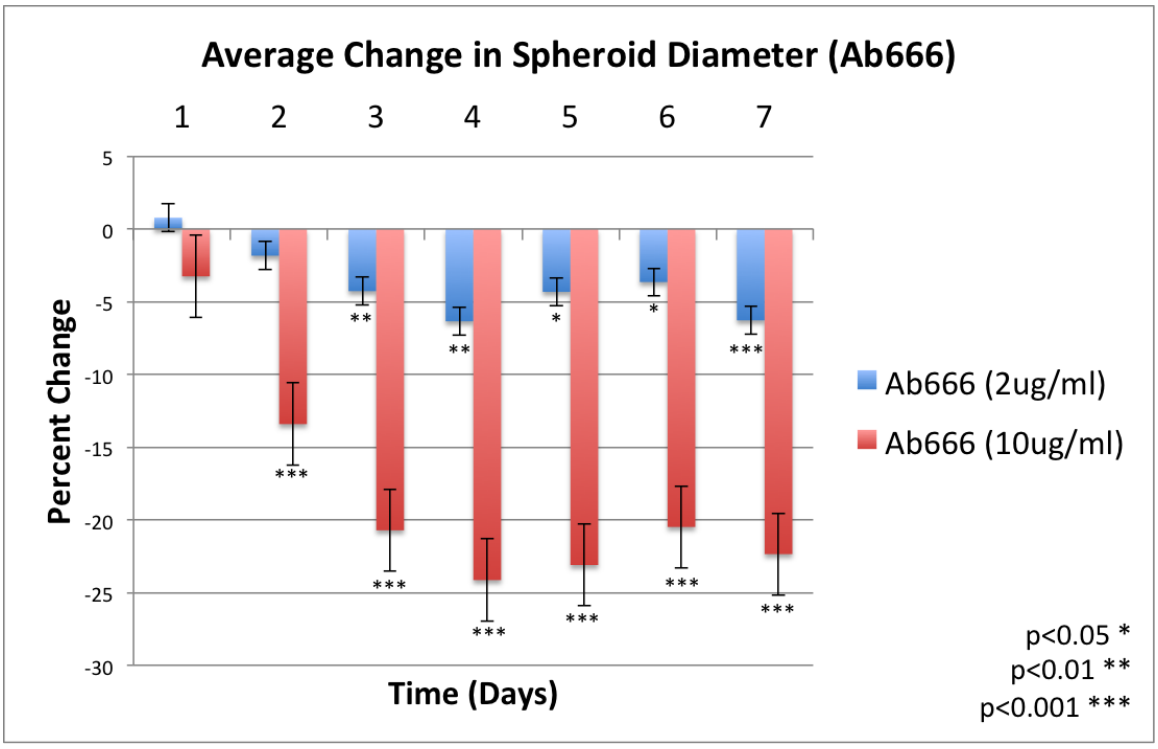

Figure 16: Average change in spheroid diameter (Ab666). U87MG cells were treated with either control culture media or anti-CD147 mAb ab666. 7 spheroids were grown for each treatment condition. Antibodies were administered at concentrations of 2 μg/ml and 10 μg/ml. Cells were grown for a total of 7 days and analyzed at 24-hours time points. Ab666 at a concentration of 10 μg/ml suppressed spheroid growth on all days after day 1. Growth was suppressed up to 24 percent of the control. A paired t-test indicated that the data from all time points was significant when compared to the control.

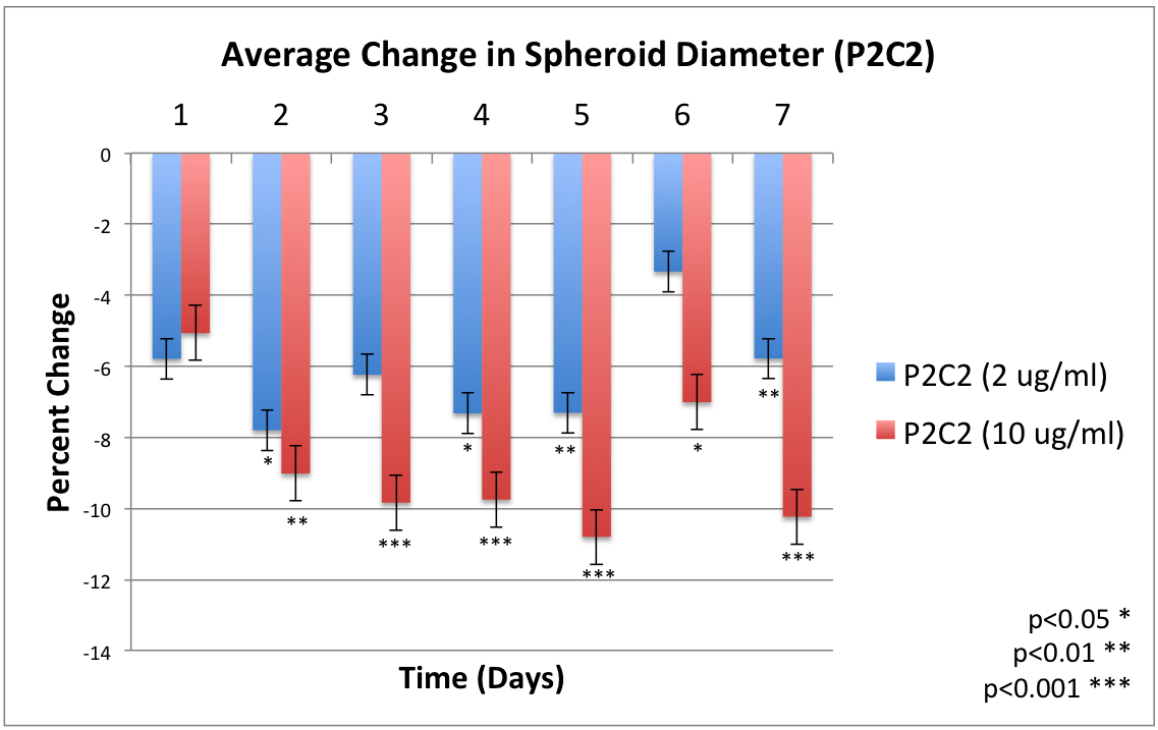

Figure 17: Average change in spheroid diameter (P2C2). U87MG cells were treated with either control culture media or anti-CD147 mAb P2C2. 7 spheroids were grown for each treatment condition. Antibodies were administered at concentrations of 2 μg/ml and 10 μg/ml. Cells were grown for a total of 7 days and analyzed at 24-hours time points. P2C2 at a concentration of 10 μg/ml suppressed spheroid growth on all days after day 1. Growth was suppressed up to 11 percent of the control. A paired t-test indicated that the data from all time points was significant when compared to the control.

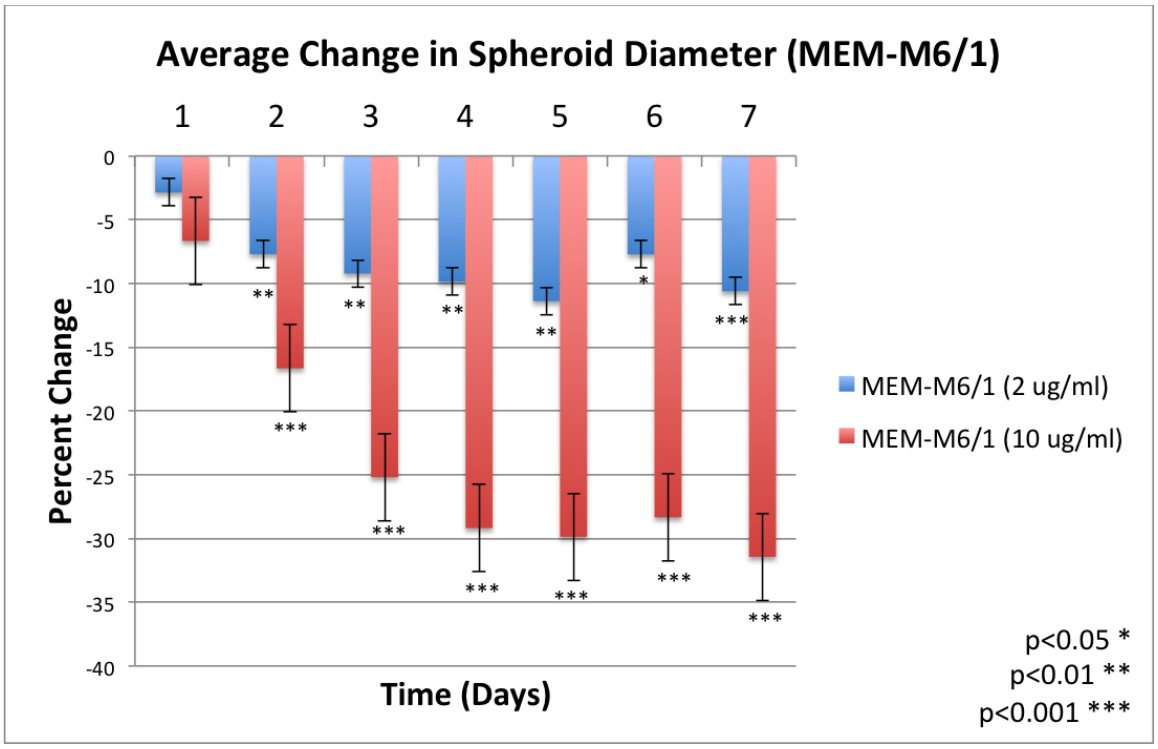

Figure 18: Average change in spheroid diameter (MEM-M6/1). U87MG cells were treated with either control culture media or anti-CD147 mAb MEM-M6/1. 7 spheroids were grown for each treatment condition. Antibodies were administered at concentrations of 2 μg/ml and 10 μg/ml. Cells were grown for a total of 7 days and analyzed at 24-hours time points. MEM-M6/1 at a concentration of 10 μg/ml suppressed spheroid growth on all days after day 1. Growth was suppressed up to 32 percent of the control. A paired t-test indicated that the data from all time points was significant when compared to the control.

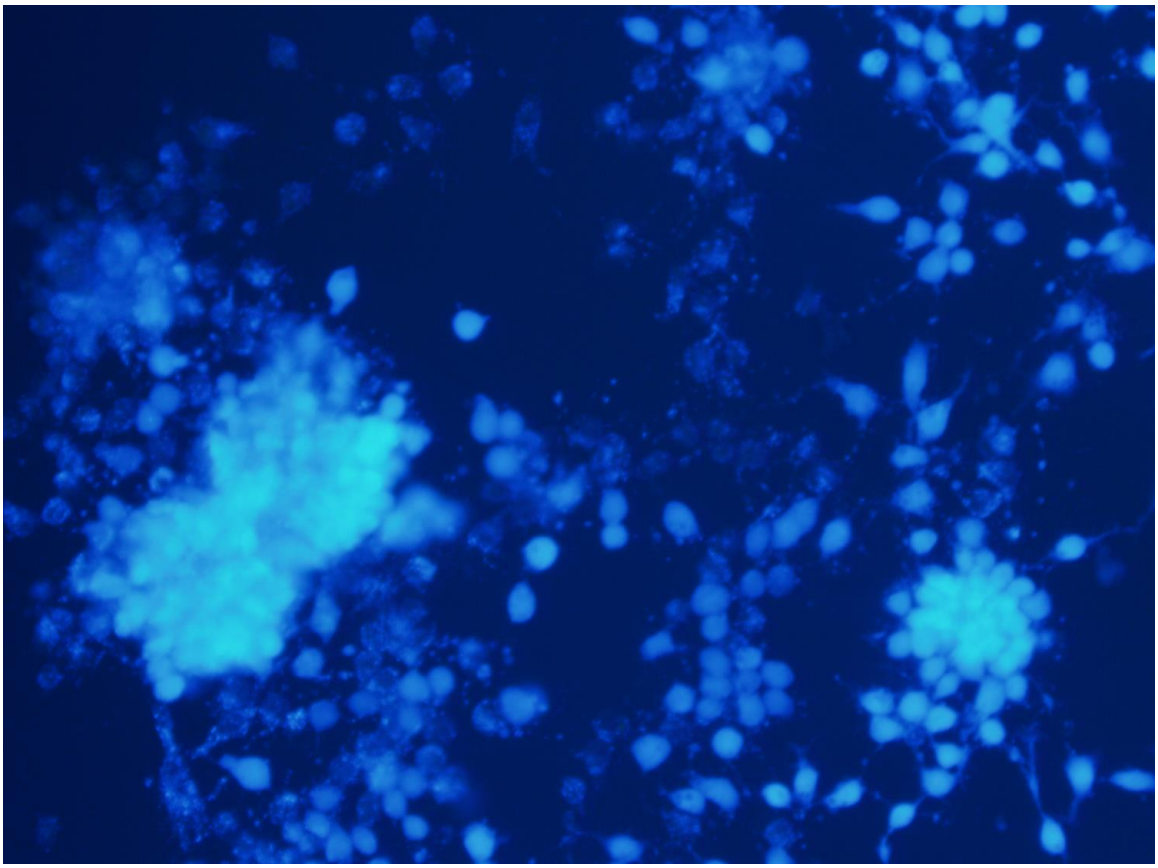

Figure 19: Positive control stained positive for live cells. U87MG cells were grown for 4 days then treated with 1 μm staurosporine in a 37(0), 5% CO2 incubator for 3.5 hours. Image shows live cells (blue, stained with CytoCalcein Violet 450). Image was taken with an Olympus DP72 fluorescence microscope through the violet channel. Data indicates the positive control contained live cells beginning to cluster.

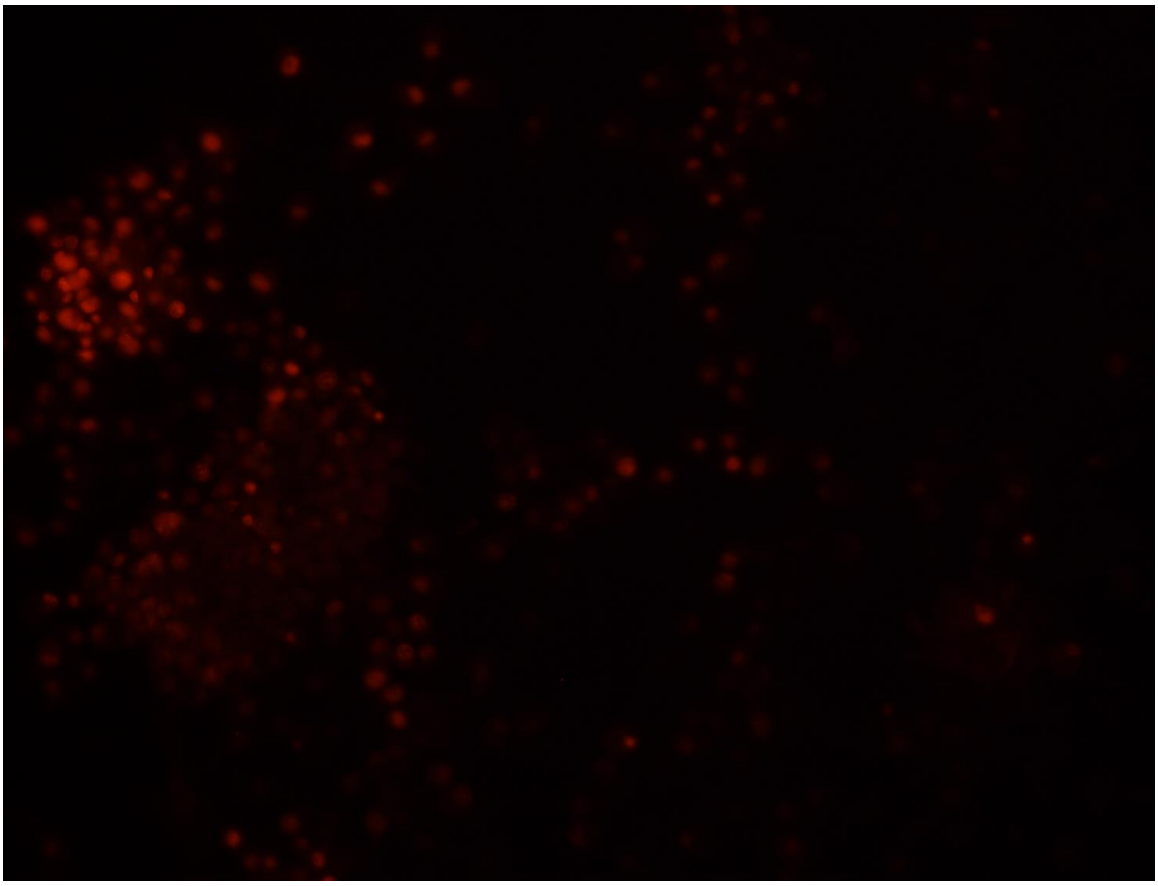

Figure 20: Positive control stained positive for apoptosis. U87MG cells were grown for 4 days then treated with 1 μm staurosporine in a 37(0), 5% CO2 incubator for 3.5 hours. Image shows apoptotic cells (red, stained with Apopxin Deep Red Indicator). Image was taken with an Olympus DP72 fluorescence microscope through the Cy5 channel. Data indicates staurosporine treatment induced apoptosis on positive control cells.

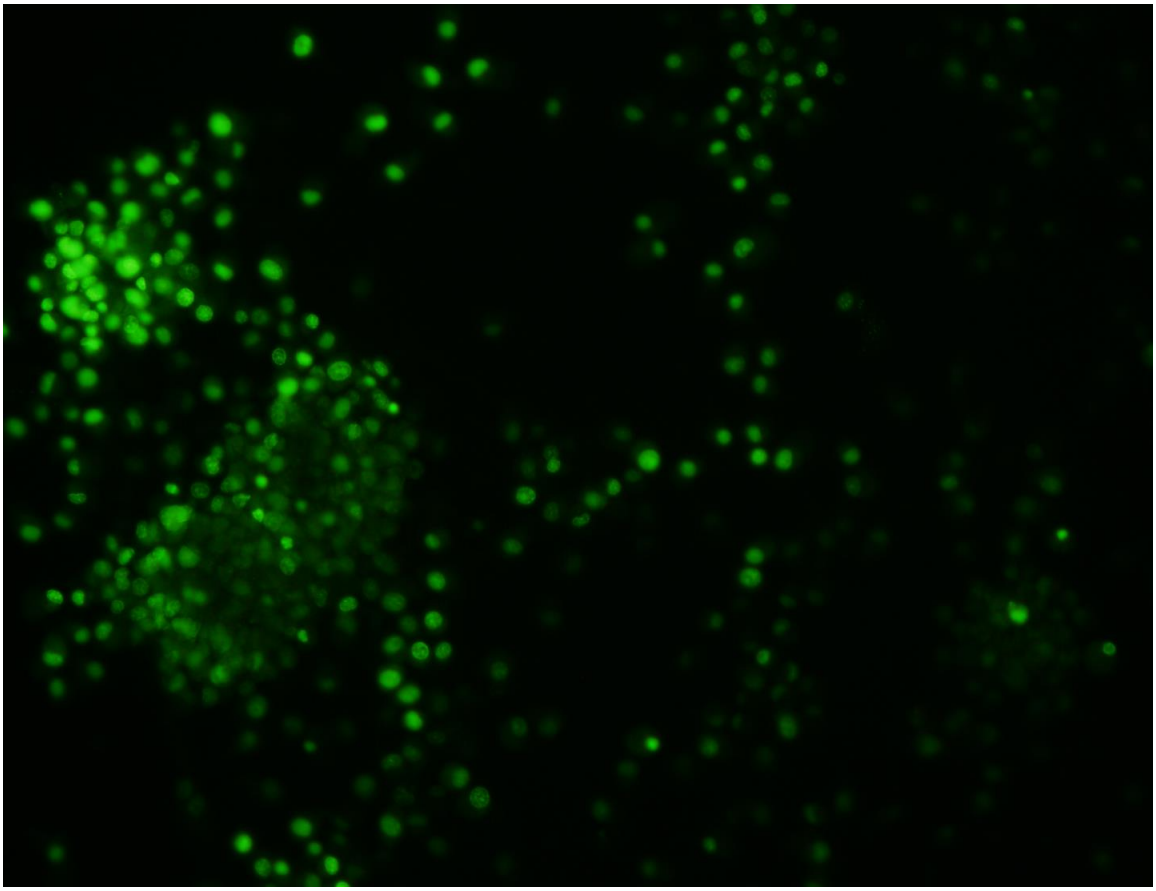

Figure 21: Positive control stained positive for necrosis. U87MG cells were grown for 4 days then treated with 1 μm staurosporine in a 37(0), 5% CO2 incubator for 3.5 hours. Image shows necrotic cells (green, stained with Nuclear Green DCS1). Image was taken with an Olympus DP72 fluorescence microscope through the FITC channel. Data indicates staurosporine treatment induced necrosis on positive control cells.

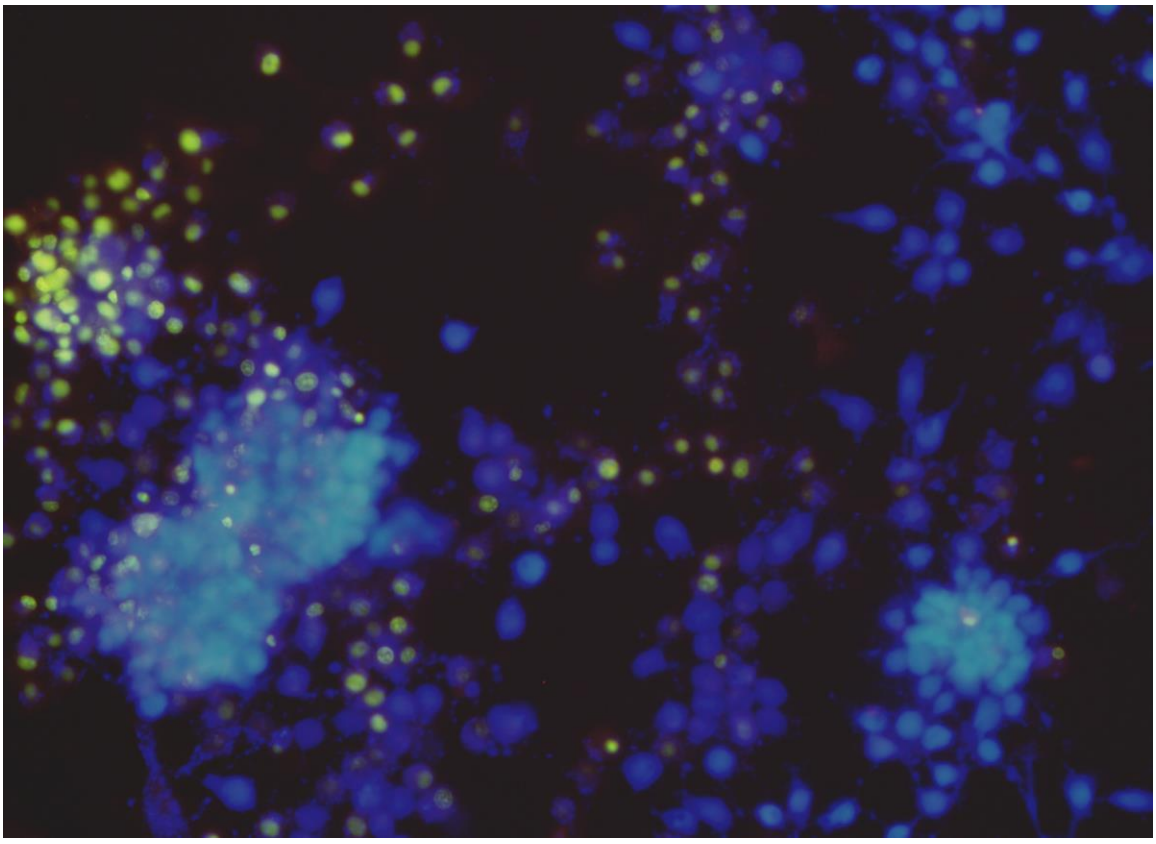

Figure 22: Positive control overlay image. U87MG cells were grown for 4 days then treated with 1 μm staurosporine in a 37(0), 5% CO2 incubator for 3.5 hours. Image shows cells that are alive (blue, stained with CytoCalcein Violet 450), apoptotic cells (red, stained with Apopxin Deep Red Indicator), and necrotic cells (green, stained with Nuclear Green DCS1). Image shows cells beginning to go through both apoptosis and necrosis due to staurosporine treatment. Overlay was produced from the same population of cells. Image was taken with an Olympus DP72 fluorescence microscope through the violet, Cy5, and FITC channel respectively.

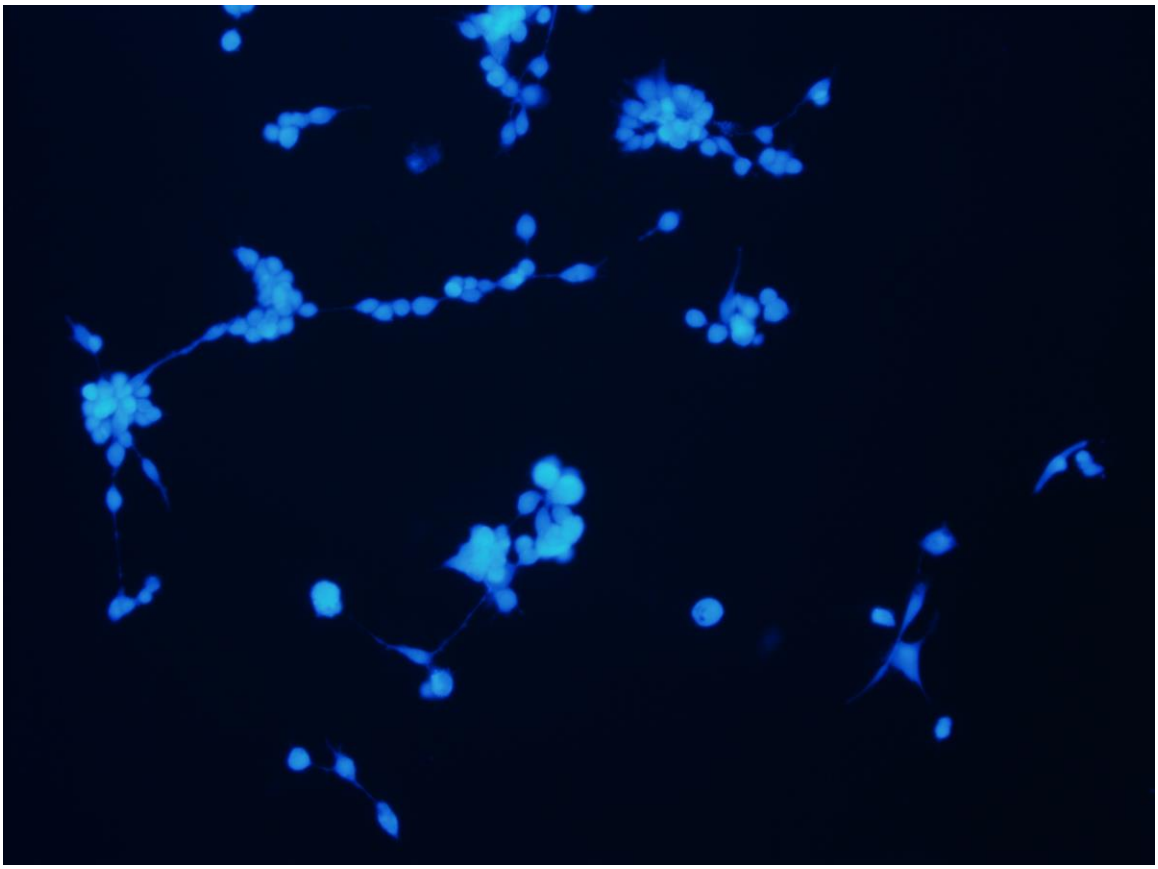

Figure 23: Negative control stained positive for live cells. Untreated U87MG cells were grown in a 37(0), 5% CO2 incubator for 4 days. Image shows live cells (blue, stained with CytoCalcein Violet 450). Image was taken with an Olympus DP72 fluorescence microscope through the violet channel. Data indicates that the negative control contained living cells.

Figure 24: Negative control stained negative for apoptosis. Untreated U87MG cells were grown in a 37(0), 5% CO2 incubator for 4 days. Cells were stained for apoptosis (red, Apopxin Deep Red Indicator). No apoptosis was detected. Image was taken with an Olympus DP72 fluorescence microscope through the Cy5 channel.

Figure 25: Negative control stained negative for necrosis. Untreated U87MG cells were grown in a 37(0), 5% CO2 incubator for 4 days. Cells were stained for necrosis (green, Nuclear Green DCS1). No necrosis was detected. Image was taken with an Olympus DP72 fluorescence microscope through the FITC channel.

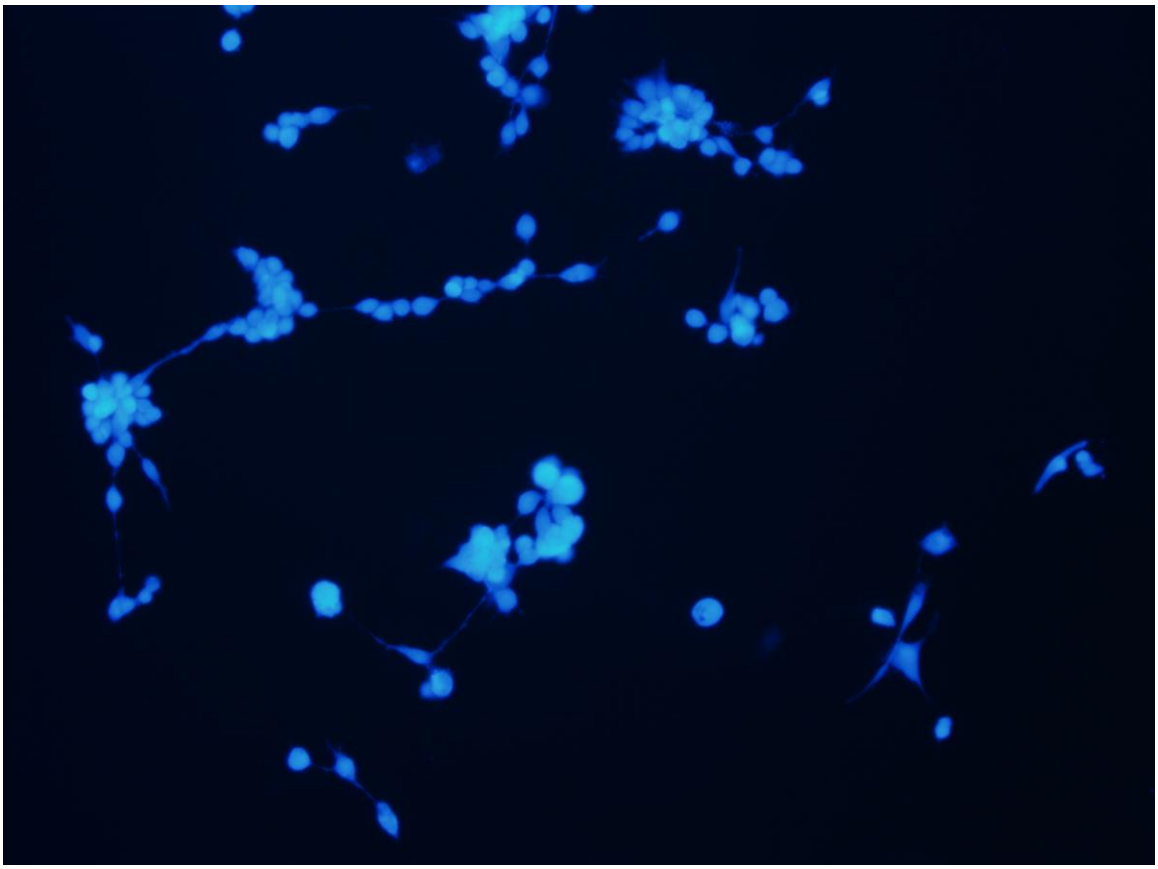

Figure 26: Negative control overlay image. Untreated U87MG cells were grown in a 37(0), 5% CO2 incubator for 4 days. Cells were stained for live cells (blue, stained with CytoCalcein Violet 450), apoptotic cells (red, stained with Apopxin Deep Red Indicator), and necrotic cells (green, stained with Nuclear Green DCS1). Image shows only live cells, indicating that the negative control cells are going through neither apoptosis nor necrosis. Overlay was produced from the same population of cells. Image was taken with an Olympus DP72 fluorescence microscope through the violet, Cy5, and FITC channel respectively.

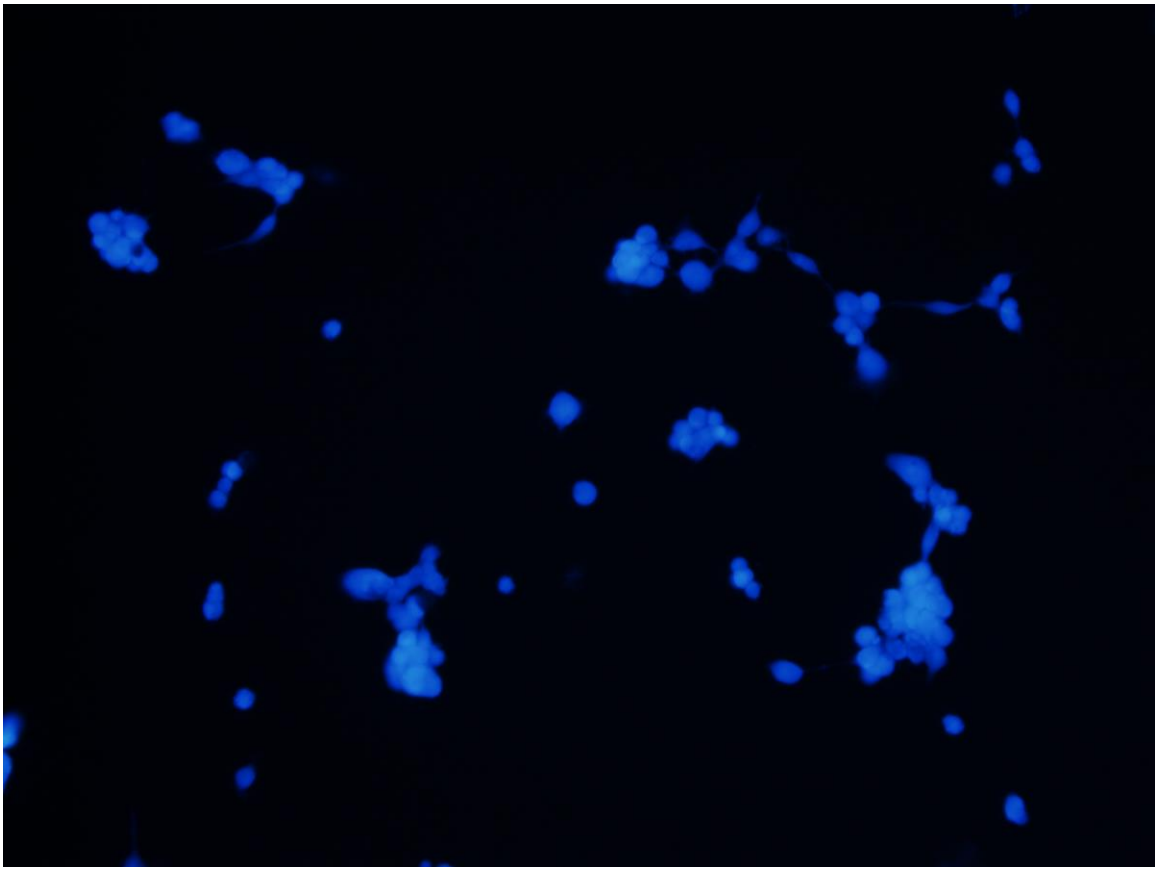

Figure 27: Anti-CD147 mAb treated cells stained positive for live cells. U87MG cells were treated with ab666 mAb (10 μg/ml) in a 37(0), 5% CO2 incubator for 4 days. Image shows live cells (blue, stained with CytoCalcein Violet 450). Image was taken with an Olympus DP72 fluorescence microscope through the violet channel.

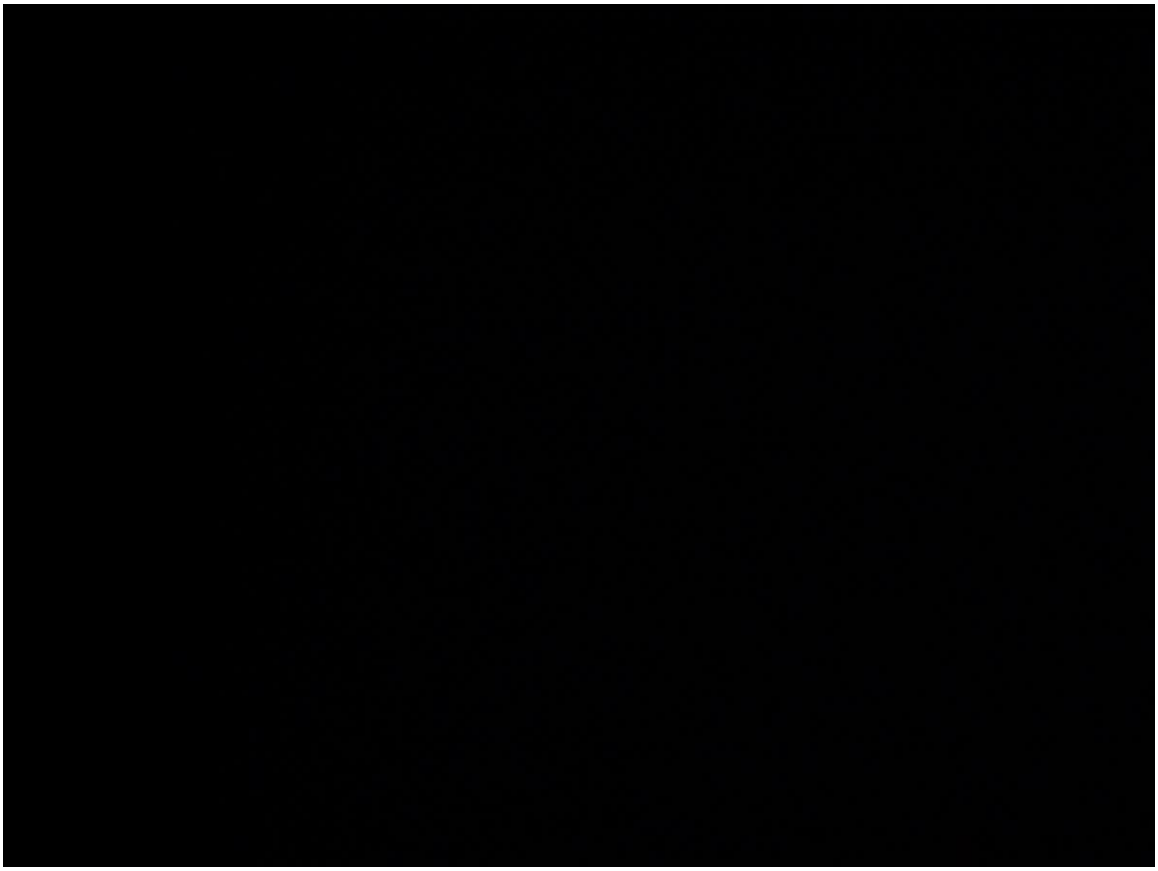

Figure 28: Anti-CD147 mAb treated cells stained negative for apoptosis. U87MG cells were treated with ab666 mAb (10 μg/ml) in a 37(0), 5% CO2 incubator for 4 days. Cells were stained for apoptosis (red, Apopxin Deep Red Indicator). No apoptosis was detected. Image was taken with an Olympus DP72 fluorescence microscope through the Cy5 channel.

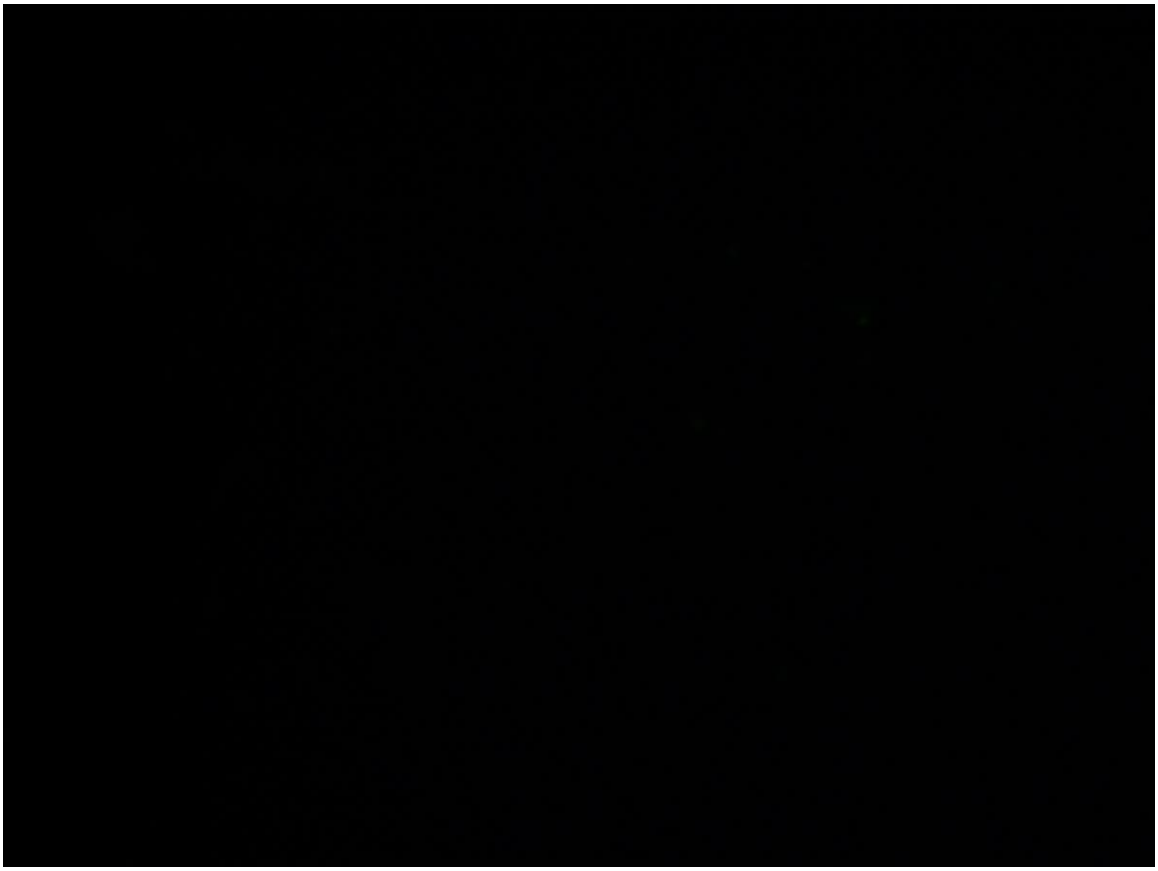

Figure 29: Anti-CD147 mAb treated cells stained negative for necrosis. U87MG cells were treated with ab666 mAb (10 μg/ml) in a 37(0), 5% CO2 incubator for 4 days. Cells were stained for necrosis (green, Nuclear Green DCS1). No necrosis was detected. Image was taken with an Olympus DP72 fluorescence microscope through the FITC channel.

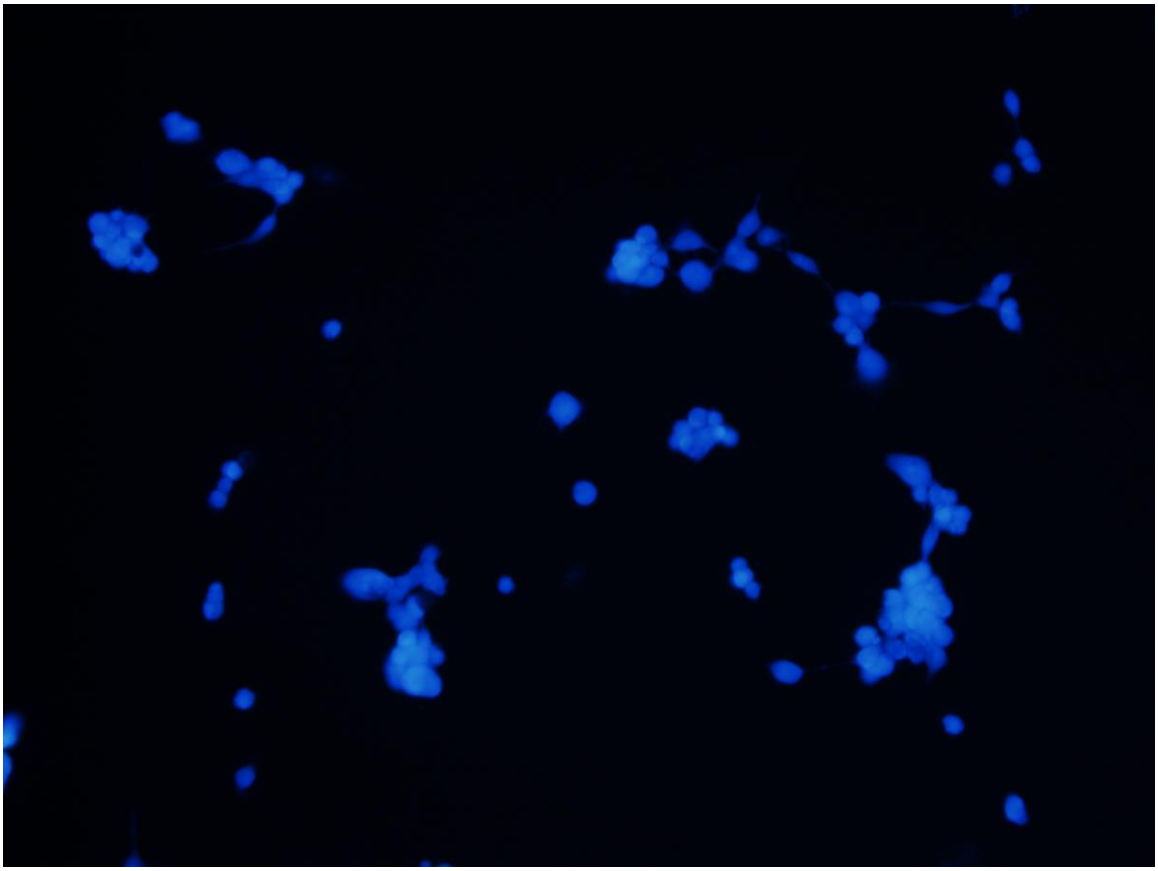

Figure 30: Anti-CD147 mAb treated cells overlay image. U87MG cells were treated with ab666 mAb (10 μg/ml) in a 37(0), 5% CO2 incubator for 4 days. Cells were stained for live cells (blue, stained with CytoCalcein Violet 450), apoptotic cells (red, stained with Apopxin Deep Red Indicator), and necrotic cells (green, stained with Nuclear Green DCS1). Image shows only live cells, indicating that the antibody treatment caused neither apoptosis nor necrosis. Overlay was produced from the same population of cells. Image was taken with an Olympus DP72 fluorescence microscope through the violet, Cy5, and FITC channel respectively.

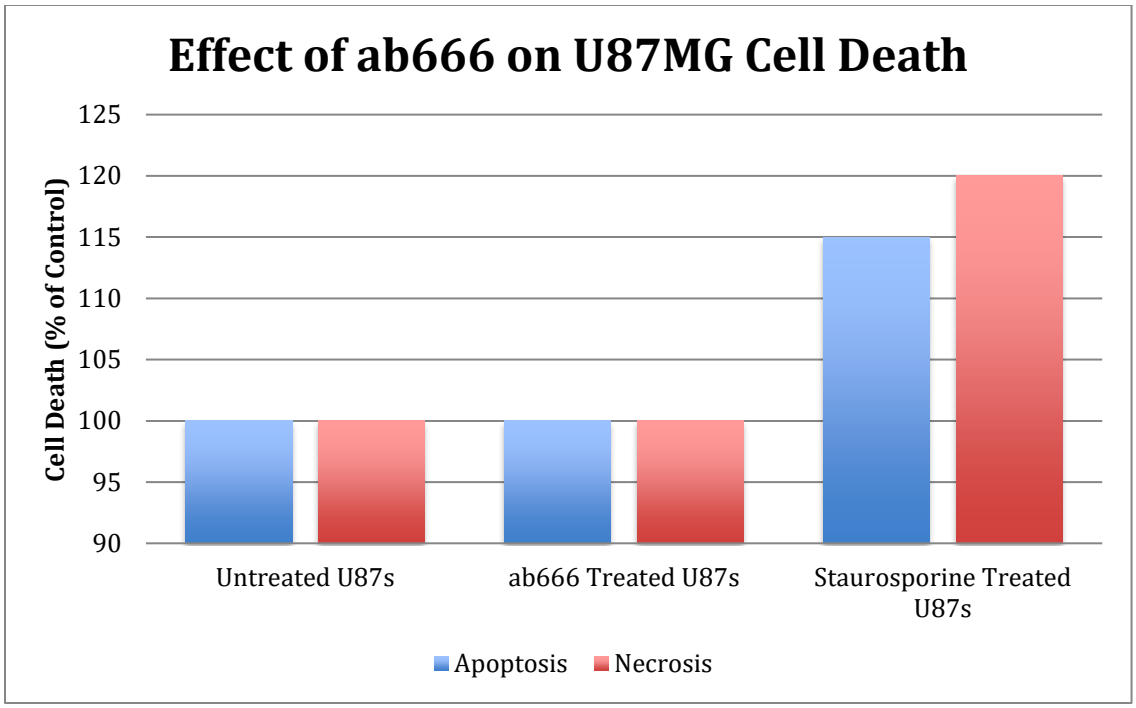

Figure 31: Anti-CD147 mAb treatment does not induce cell death. Analysis of apoptosis and necrosis on U87MG cells after 4 days in the presence of ab666 mAb (10 μg/ml), staurosporine (1 μm), or no treatment. No cell death was observed in the negative control nor the mAb treated cells. Data was expressed as percent change between control and treated samples. Apoptosis and necrosis was only detected in the positive control cells treated with 1 μm staurosporine.

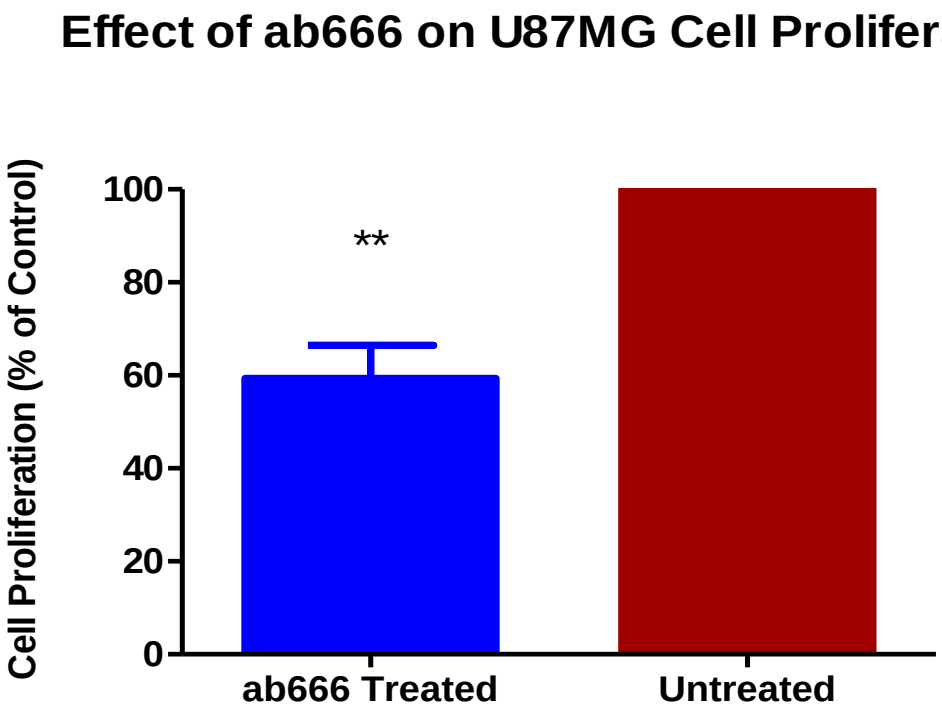

Figure 32. Anti-CD147 mAb treatment caused decreased cell proliferation. Analysis of cell proliferation in U87MG cells after 4 days of ab666 mAb treatment (10 μg/ml), or no treatment. Cell proliferation significantly decreased in the mAb treated cells. Data was expressed as percent change between control and treated samples.

DISCUSSION

While it has been shown that CD147 interference/knockdown suppresses cell growth in adherent melanoma and colon cancer cells[42], this would be a novel finding in GBM multicellular tumor spheroids. In the present work, we have shown that anti-CD147 mAbs (ab666, MEM-M6/1, & P2C2) significantly suppress U87MG spheroid growth. Previous studies have demonstrated that CD147 forms a complex with monocarboxlate transporters on the cell surface, and it seems this interaction is crucial for tumor cell survival[42]. Directly downstream of the CD147/MCT complex lies the PI3K/Akt/MDM2 pathway – an important system that controls the tumor suppressor gene p53[51]. P53 activity is increased in response to cellular stress such as DNA damage and oncogene activation[52]. The primary regulator of p53 is MDM2, which functions to inhibit p53 transcriptional activation[52]. One specific study showed that phosphorylation of Akt and MDM2 was significantly decreased when CD147 was either knocked down or knocked out[51]. Additionally, p53 levels increased when CD147 was being inhibited[51]. This highlights a direct correlation between CD147 and the PI3K/Akt/MDM2 pathway. The study also highlighted an inverse correlation between lactic acidosis and PI3K/Akt activity, showing that Akt activity was reduced by a MCT1 inhibitor[51]. Additionally, Akt activity was significantly increased in MCT1 overexpressing cells. This highlights the importance of the CD147/MCT complex in the function of the PI3K/Akt/MDM2 pathway. Specific growth factors are responsible for activation of the PI3K/Akt/MDM2

pathway, and one molecule that lays directly upstream is EGFR, a receptor tyrosine kinase. To become activated, RTKs generally require ligand binding that eventually leads to phosphorylation of the receptor. However, in cancer, RTKs can become phosphorylated in the absence of a ligand[54]. Overexpression or mutations of these receptors can lead to clustering, causing them to homodimerize and become phosphorylated. This autophosphorylation leads to constant activation of the pathway, which can eventually lead to cancer. As mentioned previously, all of this data suggests that the CD147/MCT complex along with EGFR activity play a role in activating the PI3K/Akt/MDM2 pathway. We believe that interfering with CD147 function may subsequently inhibit the PI3K/Akt/MDM2 pathway, leading to increased p53 expression and its tumor suppressing properties.

While Baba et al. reported similar findings to ours in their 2008 paper; there are key differences with our current work. Baba et al. reported that inhibiting expression of the CD147/MCT complex using mAb ab666 decreased the number of melanoma and colon cancer cells, but not normal fibroblasts[42]. While searching for the mechanism to explain this finding, an apoptosis assay was done which resulted in negative data. It was then assumed that since the hallmarks of apoptosis were not seen, the reason for decreased cell numbers was necrotic cell death. This is a major assumption because other factors could be causing this, such as an interruption of cellular metabolism leading to decreased proliferation. We investigated this possibility by using multicellular spheroids. Once cell culture conditions were optimized, multicellular tumor spheroids were grown using U87MG cells and treated with the same mAb used by Baba et al., along with two other anti-CD147 mAbs. As hypothesized, these anti-CD147 mAbs significantly

suppressed spheroid growth during the 7-day treatment. An interesting finding within these results is that two of the mAbs (ab666 & MEM-M6-1) had more significant effects on spheroid growth than the other (P2C2). In fact, the two mAbs that showed higher significance are the same mAb clone produced by different manufacturers. According to both manufacturers, this antibody clone recognizes and binds to an epitope in the N-terminal Ig domain (D1). This could be an important factor for the difference seen between the effects of the different mAbs. The site at which an antibody binds, whether extracellularly or intracellularly, could play a large role in mab effect.

In order to determine how these mAbs suppressed spheroid growth, a cell death assay for both apoptosis and necrosis was used. Using the same culture conditions, U87MG cells were grown in the presence of ab666 for four days. To test for these mechanisms of cell death, positive control cells, negative control cells, and mAb treated cells were stained with three different stains after the growth period was complete. Positive control cells are used to represent the response being tested, whereas negative control cells represent normal cells with no response. A live cell stain, an apoptosis stain, and a necrosis stain were all used in combination to test for cell death in all three culture conditions. The live stain (CytoCalcein Violet 450) works by entering the cytoplasm of live cells, where specific esterases cleave an ester group from the stain, which yields the fluorescent dye. Dead cells that have compromised cell membranes are not able to complete this process. The apoptotic stain (Apopxin Deep Red) works by binding directly to phosphatidylserine, which moves to the outside of the cell during apoptosis allowing for easy detection which is observed as red fluorescent light. Phosphatidylserine on the cell surface is a universal indicator of the early signs of apoptosis, and can be detected

before cell morphology changes drastically. The necrotic stain (Nuclear Green DCS1) is a membrane impermeable dye that enters the nucleus of cells that have lost their membrane integrity due to cellular damage and fluoresces as green light. As expected, the positive control cells treated with staurosporine, which induces cell death, stained positive for both apoptosis and necrosis. Again, as expected, the untreated negative control cells were negative for both apoptosis and necrosis staining. Like Baba et al., our mAb treated cells were negative for apoptosis staining. Our results differed, though, when it came to necrotic cell death. The mAb treated cells were also negative for necrosis staining, which raised the question of how these cells could be experiencing a decrease in cell growth.

A literature review of tumor cell proliferation was performed to find a possible clue to explain our results. We learned that the CD147/MCT complex lies directly upstream of the PI3K/Akt/MDM2 pathway[51]. We also learned that EGFR lies directly upstream of the pathway and acts as a functional regulator for PI3K/Akt/MDM2 activation[53]. Finally, it was learned that CD147 forms a complex with EGFR inside lipid rafts of the plasma membrane, which could have serious implications in our study[56]. CD147 and EGFR are both overexpressed in GBM, which leads to increased tumor cell survival by promoting cancerous properties. Since EGFR acts as a regulator for the PI3K/Akt/MDM2 pathway, its activation leads to activation of the pathway. Overexpression of EGFR may cause receptor clustering and can eventually lead to homodimerization and autophosphorylation of the receptor. This would activate the pathway in the absence of a ligand, ultimately promoting cancer. The PI3K/Akt/MDM2 pathway is critical for cellular functions such as proliferation, glucose metabolism, and

angiogenesis.

When functioning properly, p53 can inhibit the downstream effects of the PI3K/Akt/MDM2 signaling pathway in tumor cells. Using the CellQuanti-Blue proliferation assay, we analyzed the proliferation of mAb treated cells versus control cells. After growing cells in both conditions for 4 days, cells were stained with CellQuanti-Blue reagent and incubated for an hour. Following incubation, cells were analyzed for total fluorescence, which represents proliferation. Overall, the mAb treated cells had a decreased proliferation rate of nearly 40% when compared with the control. Rather than cell death, these GBM cells treated with anti-CD147 mAbs appear to experience a significant decrease in cell proliferation. Reviewing the literature gives a molecular basis for these results. Interference of the CD147/MCT/EGFR complexes has potential to cause serious problems for tumor cell survival. We believe that anti-CD147 mAb binding is causing internalization of these complexes, inhibiting their function and leading to inhibition of the PI3K/Akt/MDM2 pathway. Since these complexes carry out their functions on the cell surface, internalization into the cell would prevent them from being able to function properly. Overall, the inhibition of this pathway would remove the inhibition of tumor suppressor p53 and allow it to carry out its proper function – suppressing tumor cells.

To further analyze the effects of our different mAbs, epitope mapping of each antibody should be done to confirm exactly where each mAb is binding to its target protein. Locating the exact binding site of an antibody provides crucial information when developing a new therapeutic drug. Further analysis of the PI3K/Akt/MDM2 pathway should also be completed to confirm the hypothesis of its downstream role in tumor cell

proliferation. Following mAb treatment, cellular levels of EGFR, Akt and p53 could be measured and compared to a control. Other techniques besides mAb treatment could also be used to inhibit CD147 function, such as a true knockdown or knockout to analyze the effects it may have on this pathway.

CONCLUSION

In conclusion, we have demonstrated that anti-CD147 monoclonal antibodies suppress the growth of U87MG multicellular tumor spheroids. Furthermore, we have shown that when treated with these mAbs, U87MG cells are not undergoing apoptosis or necrosis. We have also shown that cellular proliferation is significantly decreased post antibody treatment, showing a decreased proliferation rate of nearly 40 percent when compared with control cells. It is likely that these findings are a result of the PI3K/Akt/MDM2 pathway being subsequently inhibited by CD147 interference, although further analysis will be needed to confirm this hypothesis. For future GBM treatment, we have came to two important conclusions; monoclonal antibodies can be used to target the specific CD147 protein, and CD147 is a worthwhile therapeutic target for GBM.

REFERENCES

1. Tumor Types. National Brain Tumor Society. http://braintumor.org/brain-tumor-information/understanding-brain-tumors/tumor-types/. Accessed May 6, 2018.

2. Wilson TA, Karajannis MA, Harter DH. Glioblastoma multiforme: State of the art and future therapeutics. *Surg Neurol Int*. 2014;5:64. doi:10.4103/2152-7806.132138

3. Carlsson SK, Brothers SP, Wahlestedt C. Emerging treatment strategies for glioblastoma multiforme. *EMBO Mol Med*. 2014;6(11):1359-1370. doi:10.15252/emmm.201302627

4. *About Brain Tumors: A Primer for Patients and Caregivers*. American Brain Tumor Association; 2013.

5. McMurray JS, Klostergaard J. Chapter 7 - STAT3 Signaling in Cancer: Small Molecule Intervention as Therapy? In: *Anti-Angiogenesis Drug Discovery and Development*. Elsevier; 2014:216-267. doi:10.1016/B978-0-12-803963-2.50007-7

6. Adair TH, Montani J-P. *Angiogenesis*. San Rafael (CA): Morgan & Claypool Life Sciences; 2010. http://www.ncbi.nlm.nih.gov/books/NBK53242/. Accessed May 6, 2018.

7. Zhao P, Li Q, Shi Z, et al. GSK-3β regulates tumor growth and angiogenesis in human glioma cells. *Oncotarget*. 2015;6(31):31901-31915.

8. Gerstner ER, Batchelor TT. Antiangiogenic Therapy for Glioblastoma. *Cancer J Sudbury Mass*. 2012;18(1):45-50. doi:10.1097/PPO.0b013e3182431c6f

9. Vinay DS, Ryan EP, Pawelec G, et al. Immune evasion in cancer: Mechanistic basis and therapeutic strategies. *Semin Cancer Biol*. 2015;35 Suppl:S185-S198. doi:10.1016/j.semcancer.2015.03.004

10. Tumour necrosis factor and cancer - Waters - 2013 - The Journal of Pathology - Wiley Online Library. https://onlinelibrary.wiley.com/doi/abs/10.1002/path.4188. Accessed October 2, 2018.

11. Lewis AM, Varghese S, Xu H, Alexander HR. Interleukin-1 and cancer progression: the emerging role of interleukin-1 receptor antagonist as a novel therapeutic agent in cancer treatment. *J Transl Med*. 2006;4:48. doi:10.1186/1479-5876-4-48

12. Kumari N, Dwarakanath BS, Das A, Bhatt AN. Role of interleukin-6 in cancer progression and therapeutic resistance. *Tumour Biol J Int Soc Oncodevelopmental Biol Med*. 2016;37(9):11553-11572. doi:10.1007/s13277-016-5098-7

13. Valastyan S, Weinberg RA. Tumor metastasis: molecular insights and evolving paradigms. *Cell*. 2011;147(2):275-292. doi:10.1016/j.cell.2011.09.024

14. Gupta GP, Massagué J. Cancer Metastasis: Building a Framework. *Cell*. 2006;127(4):679-695. doi:10.1016/j.cell.2006.11.001

15. Douma S, Laar T van, Zevenhoven J, Meuwissen R, Garderen E van, Peeper DS. Suppression of anoikis and induction of metastasis by the neurotrophic receptor TrkB. *Nature*. 2004;430(7003):1034-1039. doi:10.1038/nature02765

16. Gao F, Cui Y, Jiang H, et al. Circulating tumor cell is a common property of brain glioma and promotes the monitoring system. *Oncotarget*. 2016;7(44):71330-71340. doi:10.18632/oncotarget.11114

17. Chistiakov DA, Chekhonin VP. Circulating tumor cells and their advances to promote cancer metastasis and relapse, with focus on glioblastoma multiforme. *Exp Mol Pathol*. 2018;105(2):166-174. doi:10.1016/j.yexmp.2018.07.007

18. Muramatsu T. Basigin (CD147), a multifunctional transmembrane glycoprotein with various binding partners. *J Biochem (Tokyo)*. 2016;159(5):481-490. doi:10.1093/jb/mvv127

19. Yan L, Zucker S, Toole BP. Roles of the multifunctional glycoprotein, emmprin (basigin; CD147), in tumour progression. *Thromb Haemost*. 2005;93(2):199-204. doi:10.1160/TH04-08-0536

20. Hu X, Su J, Zhou Y, et al. Repressing CD147 is a novel therapeutic strategy for malignant melanoma. *Oncotarget*. 2017;8(15):25806-25813. doi:10.18632/oncotarget.15709

21. Jia L, Wang S, Zhou H, Cao J, Hu Y, Zhang J. Caveolin-1 up-regulates CD147 glycosylation and the invasive capability of murine hepatocarcinoma cell lines. *Int J Biochem Cell Biol*. 2006;38(9):1584-1593. doi:10.1016/j.biocel.2006.03.019

22. Belton RJ, Chen L, Mesquita FS, Nowak RA. Basigin-2 Is a Cell Surface Receptor for Soluble Basigin Ligand. *J Biol Chem*. 2008;283(26):17805-17814. doi:10.1074/jbc.M801876200

23. Gabison EE, Hoang-Xuan T, Mauviel A, Menashi S. EMMPRIN/CD147, an MMP modulator in cancer, development and tissue repair. *Biochimie*. 2005;87(3-4):361-368. doi:10.1016/j.biochi.2004.09.023

24. Coste I, Gauchat JF, Wilson A, et al. Unavailability of CD147 leads to selective erythrocyte trapping in the spleen. *Blood*. 2001;97(12):3984-3988.

25. Enhancement of CD147 on M1 macrophages induces differentiation of Th17 cells in the lung interstitial fibrosis - ScienceDirect. https://www.sciencedirect.com/science/article/pii/S0925443914001732?via%3Dihub. Accessed August 11, 2018.

26. Igakura T, Kadomatsu K, Kaname T, et al. A null mutation in basigin, an immunoglobulin superfamily member, indicates its important roles in peri-implantation development and spermatogenesis. *Dev Biol*. 1998;194(2):152-165.

27. Naruhashi K, Kadomatsu K, Igakura T, et al. Abnormalities of Sensory and Memory Functions in Mice LackingBsgGene. *Biochem Biophys Res Commun*. 1997;236(3):733-737. doi:10.1006/bbrc.1997.6993

28. Yao H, Teng Y, Sun Q, et al. Important Functional Roles of Basigin in Thymocyte Development and T cell Activation. *Int J Biol Sci*. 2013;10(1):43-52. doi:10.7150/ijbs.6818

29. Biegler B, Kasinrerk W. Reduction of CD147 surface expression on primary T cells leads to enhanced cell proliferation. *Asian Pac J Allergy Immunol*. 2012;30(4):259-267.

30. Hu J, Dang N, Yao H, et al. Involvement of HAb18G/CD147 in T cell activation and immunological synapse formation. *J Cell Mol Med*. 2010;14(8):2132-2143. doi:10.1111/j.1582-4934.2010.01012.x

31. Ruiz S, Castro-Castro A, Bustelo XR. CD147 inhibits the nuclear factor of activated T-cells by impairing Vav1 and Rac1 downstream signaling. *J Biol Chem*. 2008;283(9):5554-5566. doi:10.1074/jbc.M708566200

32. Gu J, Zhang C, Chen R, et al. Clinical implications and prognostic value of EMMPRIN/CD147 and MMP2 expression in pediatric gliomas. *Eur J Pediatr*. 2009;168(6):705-710. doi:10.1007/s00431-008-0828-5

33. Xiong L, Edwards CK, Zhou L. The biological function and clinical utilization of CD147 in human diseases: a review of the current scientific literature. *Int J Mol Sci*. 2014;15(10):17411-17441. doi:10.3390/ijms151017411

34. Tsai W-C, Chen Y, Huang L-C, et al. EMMPRIN expression positively correlates with WHO grades of astrocytomas and meningiomas. *J Neurooncol*. 2013;114(3):281-290. doi:10.1007/s11060-013-1184-5

35. Tang Y, Nakada MT, Kesavan P, et al. Extracellular matrix metalloproteinase inducer stimulates tumor angiogenesis by elevating vascular endothelial cell growth factor and matrix metalloproteinases. *Cancer Res*. 2005;65(8):3193-3199. doi:10.1158/0008-5472.CAN-04-3605

36. Khayati F, Pérez-Cano L, Maouche K, et al. EMMPRIN/CD147 is a novel coreceptor of VEGFR-2 mediating its activation by VEGF. *Oncotarget*. 2015;6(12):9766-9780. doi:10.18632/oncotarget.2870

37. Agrawal SM, Yong VW. The many faces of EMMPRIN - roles in neuroinflammation. *Biochim Biophys Acta*. 2011;1812(2):213-219. doi:10.1016/j.bbadis.2010.07.018

38. Curtin KD, Meinertzhagen IA, Wyman RJ. Basigin (EMMPRIN/CD147) interacts with integrin to affect cellular architecture. *J Cell Sci*. 2005;118(12):2649-2660. doi:10.1242/jcs.02408

39. Agrawal SM, Williamson J, Sharma R, et al. Extracellular matrix metalloproteinase inducer shows active perivascular cuffs in multiple sclerosis. *Brain J Neurol*. 2013;136(Pt 6):1760-1777. doi:10.1093/brain/awt093

40. Yurchenko V, Constant S, Eisenmesser E, Bukrinsky M. Cyclophilin-CD147 interactions: a new target for anti-inflammatory therapeutics. *Clin Exp Immunol*. 2010;160(3):305-317. doi:10.1111/j.1365-2249.2010.04115.x

41. Jin ZG, Melaragno MG, Liao DF, et al. Cyclophilin A is a secreted growth factor induced by oxidative stress. *Circ Res*. 2000;87(9):789-796.

42. Baba M, Inoue M, Itoh K, Nishizawa Y. Blocking CD147 induces cell death in cancer cells through impairment of glycolytic energy metabolism. *Biochem Biophys Res Commun*. 2008;374(1):111-116. doi:10.1016/j.bbrc.2008.06.122

43. Walters DK, Arendt BK, Jelinek DF. CD147 regulates the expression of MCT1 and lactate export in multiple myeloma cells. *Cell Cycle Georget Tex*. 2013;12(19):3175-3183. doi:10.4161/cc.26193

44. Voss DM, Spina R, Carter DL, Lim KS, Jeffery CJ, Bar EE. Disruption of the monocarboxylate transporter-4-basigin interaction inhibits the hypoxic response, proliferation, and tumor progression. *Sci Rep*. 2017;7(1):4292. doi:10.1038/s41598-017-04612-w

45. Kennedy KM, Dewhirst MW. Tumor metabolism of lactate: the influence and therapeutic potential for MCT and CD147 regulation. *Future Oncol Lond Engl*. 2010;6(1):127-148. doi:10.2217/fon.09.145

46. Fink SL, Cookson BT. Apoptosis, pyroptosis, and necrosis: mechanistic description of dead and dying eukaryotic cells. *Infect Immun*. 2005;73(4):1907-1916. doi:10.1128/IAI.73.4.1907-1916.2005

47. Creagh EM, Conroy H, Martin SJ. Caspase-activation pathways in apoptosis and immunity. *Immunol Rev*. 2003;193:10-21.

48. Martin SJ, Finucane DM, Amarante-Mendes GP, O'Brien GA, Green DR. Phosphatidylserine Externalization during CD95-induced Apoptosis of Cells and Cytoplasts Requires ICE/CED-3 Protease Activity. *J Biol Chem*. 1996;271(46):28753-28756. doi:10.1074/jbc.271.46.28753

49. Hankins HM, Baldridge RD, Xu P, Graham TR. Role of flippases, scramblases and transfer proteins in phosphatidylserine subcellular distribution. *Traffic Cph Den*. 2015;16(1):35-47. doi:10.1111/tra.12233

50. Syntichaki P, Tavernarakis N. Death by necrosis. *EMBO Rep*. 2002;3(7):604-609. doi:10.1093/embo-reports/kvf138

51. Huang Q, Li J, Xing J, et al. CD147 promotes reprogramming of glucose metabolism and cell proliferation in HCC cells by inhibiting the p53-dependent signaling pathway. *J Hepatol*. 2014;61(4):859-866. doi:10.1016/j.jhep.2014.04.035

52. Shi D, Gu W. Dual Roles of MDM2 in the Regulation of p53: Ubiquitination Dependent and Ubiquitination Independent Mechanisms of MDM2 Repression of p53 Activity. *Genes Cancer*. 2012;3(3-4):240-248. doi:10.1177/1947601912455199

53. Wee P, Wang Z. Epidermal Growth Factor Receptor Cell Proliferation Signaling Pathways. *Cancers*. 2017;9(5). doi:10.3390/cancers9050052

54. Guo G, Gong K, Wohlfeld B, Hatanpaa KJ, Zhao D, Habib AA. Ligand-independent EGFR signaling. *Cancer Res*. 2015;75(17):3436-3441. doi:10.1158/0008-5472.CAN-15-0989

55. Montano N, Cenci T, Martini M, et al. Expression of EGFRvIII in Glioblastoma: Prognostic Significance Revisited. *Neoplasia N Y N*. 2011;13(12):1113-1121.

56. Grass GD, Tolliver LB, Bratoeva M, Toole BP. CD147, CD44, and the Epidermal Growth Factor Receptor (EGFR) Signaling Pathway Cooperate to Regulate Breast Epithelial Cell Invasiveness. *J Biol Chem*. 2013;288(36):26089-26104. doi:10.1074/jbc.M113.497685

57. Fennema E, Rivron N, Rouwkema J, van Blitterswijk C, de Boer J. Spheroid culture as a tool for creating 3D complex tissues. *Trends Biotechnol*. 2013;31(2):108-115. doi:10.1016/j.tibtech.2012.12.003

58. Zanoni M, Piccinini F, Arienti C, et al. 3D tumor spheroid models for *in vitro* therapeutic screening: a systematic approach to enhance the biological relevance of data obtained. *Sci Rep*. 2016;6:19103. doi:10.1038/srep19103

59. Antoni D, Burckel H, Josset E, Noel G. Three-dimensional cell culture: a breakthrough in vivo. *Int J Mol Sci*. 2015;16(3):5517-5527. doi:10.3390/ijms16035517

APPENDIX A

License to use Figure 1 from "Understanding the Warburg effect: the metabolic requirements of cell proliferation" by Heiden et al. received from The American Association for the Advancement of Science.

License Number	4456811199596
License date	Oct 26, 2018
Licensed Content Publisher	The American Association for the Advancement of Science
Licensed Content Publication	Science
Licensed Content Title	Understanding the Warburg Effect: The Metabolic Requirements of Cell Proliferation
Licensed Content Author	Matthew G. Vander Heiden,Lewis C. Cantley,Craig B. Thompson
Licensed Content Date	May 22, 2009
Licensed Content Volume	324
Licensed Content Issue	5930
Volume number	324
Issue number	5930
Type of Use	Thesis / Dissertation
Requestor type	Scientist/individual at a research institution
Format	Electronic
Portion	Text Excerpt
Number of pages requested	1
Order reference number	
Title of your thesis / dissertation	CD147 As A Potential Therapeutic Target In Glioblastoma
Expected completion date	Nov 2018
Estimated size(pages)	70

APPENDIX B

License to use Figure 2 from "CD147 promotes reprogramming of glucose metabolism and cell proliferation in HCC cells by inhibiting the p53-dependent signaling pathway" by Huang et al. received from Elsevier Publishing.

License Number	4456820042677
License date	Oct 26, 2018
Licensed Content Publisher	Elsevier
Licensed Content Publication	Journal of Hepatology
Licensed Content Title	CD147 promotes reprogramming of glucose metabolism and cell proliferation in HCC cells by inhibiting the p53-dependent signaling pathway
Licensed Content Author	Qichao Huang,Jibin Li,Jinliang Xing,Weiwei Li,Hongwei Li,Xia Ke,Jing Zhang,Tingting Ren,Yukui Shang,Hushan Yang,Jianli Jiang,Zhinan Chen
Licensed Content Date	Oct 1, 2014
Licensed Content Volume	61
Licensed Content Issue	4
Licensed Content Pages	8
Start Page	859
End Page	866
Type of Use	reuse in a thesis/dissertation
Intended publisher of new work	other
Portion	figures/tables/illustrations
Number of figures/tables/illustrations	1
Format	electronic
Are you the author of this Elsevier article?	No
Will you be translating?	No
Original figure numbers	Figure 4f
Title of your thesis/dissertation	CD147 As A Potential Therapeutic Target In Glioblastoma
Expected completion date	Nov 2018
Estimated size (number of pages)	70